OPTIMAL NON-COPLANAR LAUNCH TO QUICK RENDEZVOUS

THESIS

Gregory B. Sears, Captain, USAF

AFIT/GSO/ENY/97D-03

DEPARTMENT OF THE AIR FORCE
AIR UNIVERSITY
AIR FORCE INSTITUTE OF TECHNOLOGY

Wright-Patterson Air Force Base, Ohio

AFIT/GSO/ENY/97D-03

OPTIMAL NON-COPLANAR LAUNCH TO QUICK RENDEZVOUS

THESIS

Gregory B. Sears, Captain, USAF

AFIT/GSO/ENY/97D-03

The views expressed in this thesis are those of the author and do not reflect the official policy or position of the Department of Defense or the U.S. Government.

AFIT/GSO/ENY/97D-03

OPTIMAL NON-COPLANAR LAUNCH TO QUICK RENDEZVOUS

THESIS

Presented to the Faculty of the School of Engineering

of the Air Force Institute of Technology

Air University

Air Education and Training Command

In Partial Fulfillment of the Requirements for the

Degree of Master of Science in Space Operations

Gregory B. Sears, B.S.

Captain, USAF

December 1997

AFIT/GSO/ENY/97D-03

OPTIMAL NON-COPLANAR LAUNCH TO QUICK RENDEZVOUS

Gregory B. Sears, B.S.
Captain, USAF

Approved:

William E. Wiesel

Dr. William E. Wiesel
Professor of Astronautics
Thesis Advisor

1 Dec 97
date

Sharon A. Heise

Captain Sharon Heise, USAF
Assistant Professor of Aerospace Engineering
Committee Member

1 DEC 97
date

Bradley S. Liebst

Dr. Bradley S. Liebst
Associate Professor of Aerospace Engineering
Committee Member

1 Dec 97
date

Acknowledgments

I would like to thank my advisor, Dr. William Wiesel, for allowing me to work on this research with him. By sharing his knowledge, patience, and sense of humor with me, he made a long and difficult process enjoyable. I would like to thank the United States Air Force for affording me all of the opportunities and experiences of AFIT. Finally, and most important, I would like to thank my family, especially my wife Julie, and children, Stephen and Abigail. Without their love, support, and understanding, you would not be reading these pages.

Table of Contents

List of Figures

List of Tables

Abstract

The purpose of this study was to determine the feasibility of launching a Delta Clipper-like vehicle on an optimal, non-coplanar trajectory to rendezvous with an earth orbiting object in one orbit or less. The focus of the research was to determine what such a trajectory would look like, and to determine the cost, in payload mass, of flying such a trajectory. A model for the ascent trajectory was developed using the dynamics equations of motion, an atmosphere model, and an aerodynamic model for the DC-Y concept vehicle. A boundary value problem was posed and solved for a coplanar rendezvous. The non-coplanar solutions were obtained through extrapolation from the coplanar solution.

OPTIMAL NON-COPLANAR LAUNCH TO QUICK REDEZVOUS

I. INTRODUCTION

1.1 Motivation

The motivation for this research was to take a new look at the way space vehicles are launched to rendezvous with satellites and/or space stations. Current practice is to set launch windows based on the time the desired orbital plane passes over the launch facility. Once the vehicle is in orbit, a game of catch-up is played for a day or two until the rendezvous occurs. The tradeoff for such restricted time schedules is that this is a minimum energy method that minimizes fuel requirements and maximizes the mass of the vehicle and the payload being sent to orbit. The new designs and concepts for single stage to orbit (SSTO) vehicles and 'space planes', as well as the increased presence of potential rendezvous 'targets' (i.e. space station, troubled satellite etc.), has prompted the search for a more flexible way to rendezvous with orbiting objects. Specifically, could a launch method be developed with the ability to access a range of orbital planes that set the launch time to match the phase of the approaching target and allowing us to pop-up next to the 'target' at burnout? If this could be achieved, how much payload mass would it cost to follow such a rendezvous trajectory? This capability could offer a solution to emergency repair or re-supply situations as well as a variety of other applications that are left for speculation by the reader.

1.2 Overview

The rest of this chapter is devoted to the background and description of the DC-Y concept vehicle. Chapter 2 describes the set up of the problem, as well as the various factors that need to be accounted for in this problem. Chapter 2 also begins the derivation of the equations of motion. The equations of motion are completed, the optimality conditions are derived, and the boundary value problem is posed in Chapter 3. In Chapter 4, the computer algorithms are discussed, and the coplanar case is solved and extrapolated to provide the non-coplanar solutions for several different cases. The results for a non-aerodynamic scenario are presented in Chapter 5 and a gravity turn scenario in Chapter 6. Finally, conclusions and recommendations are presented in Chapter 7.

1.3 Background

In 1990, The Ballistic Missile Defense Organization (BMDO) began investigating the feasibility of SSTO vehicles. After considering multiple design concepts, McDonnell Douglas was awarded the contract to develop and test their Delta Clipper Experimental Launch Vehicle (DC-X) in 1991. This design was a vertical take-off, vertical landing (VTVL) concept that launched vertically and after reaching orbit and delivering its payload, would reenter the atmosphere nose down. It could be controlled through the use of body flaps and at a specified point in the reentry, would perform a rotation to base first and land in the same orientation from which it launched. Under the guidance of the Air Force's Phillips Laboratory, the first DC-X test flight at White Sands Missile Range occurred only 24 months after BMDO authorized McDonnell Douglas to proceed with

the development. Unfortunately, BMDO's mission was modified to dealing with only ground-based missile defense and their involvement with SSTO technologies ended with the test flight. Currently, NASA is proceeding with development of SSTO vehicles under the X-33 program. Unfortunately, the DC-X-type designs have been eliminated from the design options for the X-33.

The vehicle modeled in this research is a modification to the DC-X termed the DC-Y. It is essentially a larger version of the tested DC-X that still follows the VTVL philosophy, and is basically conical in shape. Four large and four smaller engines, all of which use LH_2/LO_2 for propellant, power it. In addition, there is also a gaseous oxygen-hydrogen reaction control system used to control the roll of the vehicle. Table 1-1 lists some of the statistics for the DC-Y. Figure 1-1 gives a diagram of both the DC-X and DC-Y vehicles that was downloaded from a McDonnell Douglas web site, which no longer exists. The quality is not the best, but it gives a good idea of what the two vehicles look like. In addition, Figure 1-2 gives some different views of the vehicle, which, for a while, was an X-33 design candidate

Table 1-1. DC-Y Statistics

Length	127 ft.
Width	18 ft.
Dry Weight	104,000 lbs.
Loaded Weight	1,279,000 lbs.
Thrust to Weight Ratio	1.4
Specific Impulse (I_{sp})	450 sec.

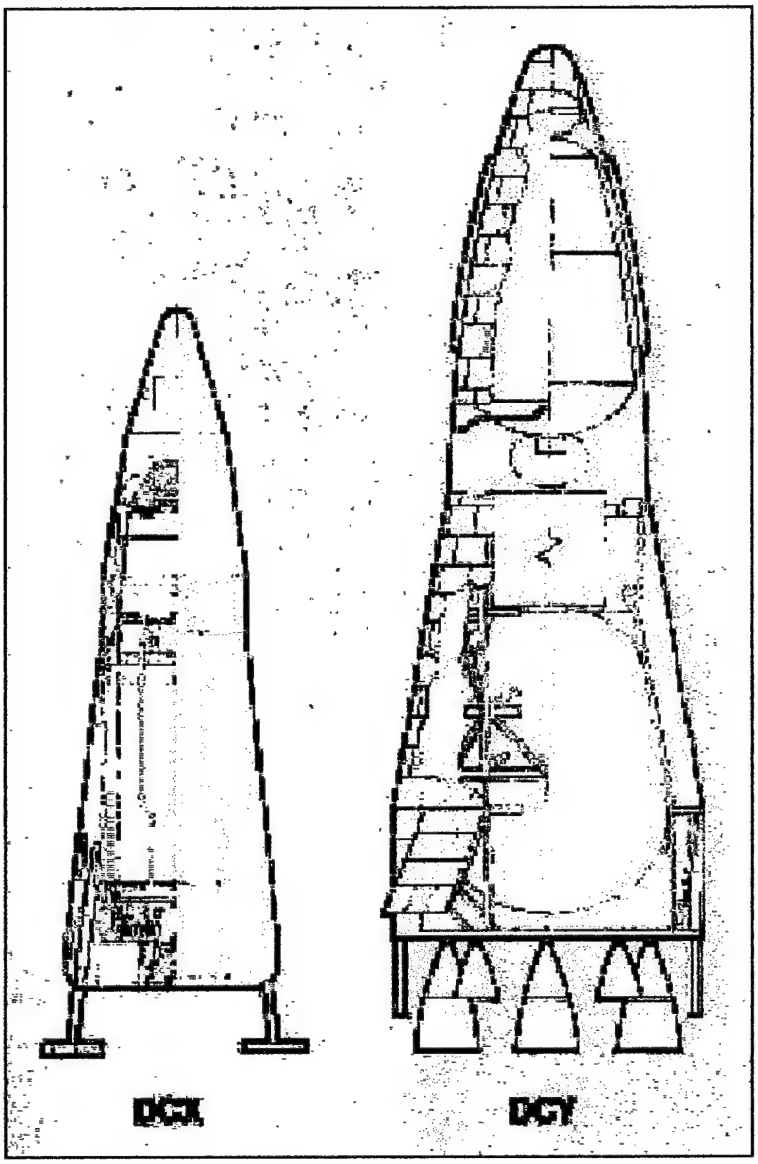

Figure 1-1. DC-X and DC-Y Designs

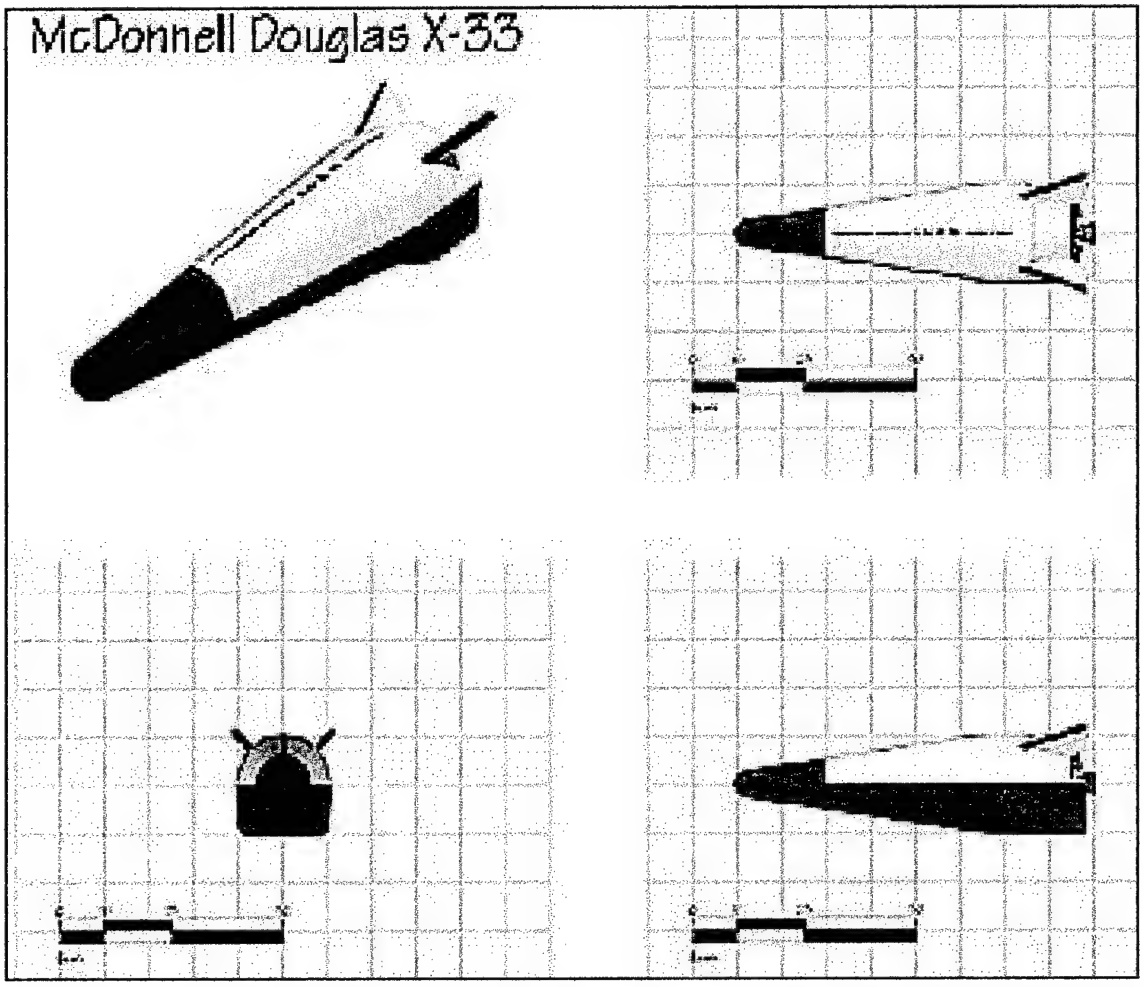

Figure 1-2. Views of the DC-Y

The major motivating factor for choosing the DC-Y design as the model for this research was the excellent lift to drag ratio this design possesses. Since we will be allowing the vehicle to have an angle of attack along the trajectory, the higher this lift to drag ratio, the better. Figure 1-3, shows the coefficients of lift and drag versus angle of attack from data obtained for the DC-Y design.

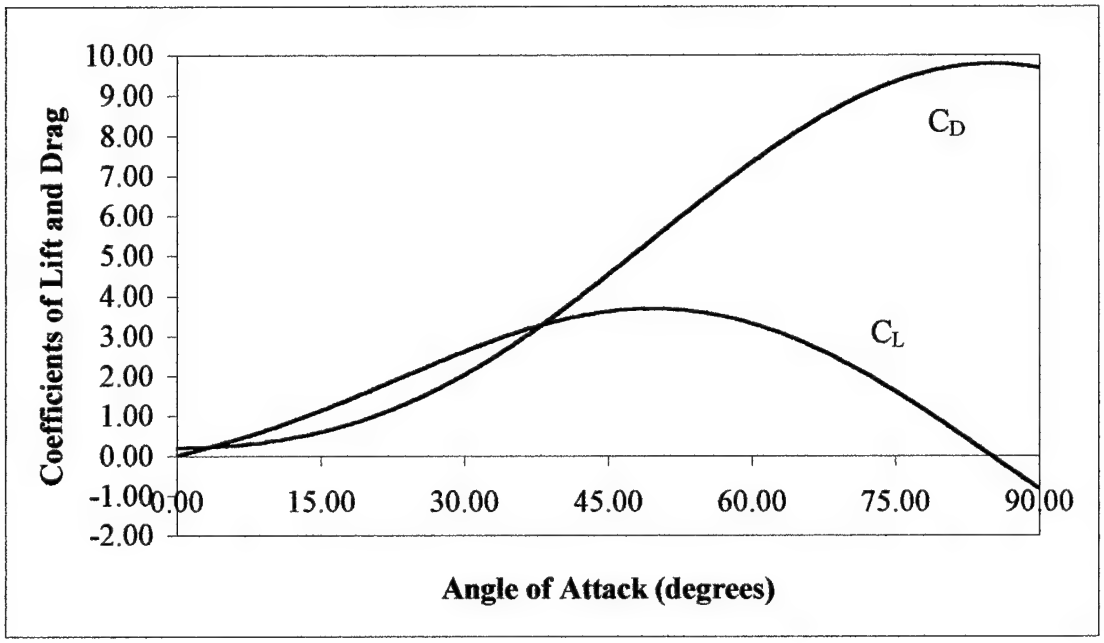

Figure 1-3. C_L and C_D vs. Angle of Attack for DC-Y

Now that we have an understanding of the vehicle used in this research, we can proceed to the next chapter and begin setting up the problem.

II. MODELING THE TRAJECTORY

2.1 Literature Search

A search of the current literature resulted in finding articles about the DC-X program and plane change maneuvers that could be performed once a coplanar launch trajectory had been followed. However, no articles or papers were found that discussed launching on a trajectory that would result in a direct insertion into a non-coplanar orbit.

2.2 Reference Frames

Development of the equations of motion is a modification of the development presented in Vinh[6, 21-27]. The modifications made for this problem are: roll is defined positive to the right, and the heading angle is defined positive from the north. These angles will be defined shortly.

The first step is to establish the reference frames necessary to set up the problem. The requirements for this problem are such that a geocentric inertial reference frame (X,Y,Z) is sufficient. This reference frame is fixed with respect to the earth and is rotating with constant angular velocity $\vec{\omega}$ about the Z-axis. Three quantities in the inertial frame are required to specify the vehicle's position. These quantities are:

1. r, the magnitude of the position vector measured from the center of the earth
2. θ, longitude measured positive eastward from the X-axis in the equatorial plane
3. ϕ, latitude measured positive northward from the equator along a meridian.

Next, it is convenient to develop the dynamics of this system in a frame which is rotating with respect to the center of the earth (x,y,z). The x-axis is defined along the position vector (up), the y-axis is in the earth's equatorial plane and is orthogonal to the x-axis

(east), and the z-axis is such that it completes the right-handed coordinate system, orthogonal to both the x-axis and y-axis (north). The local horizontal plane is defined as the plane that passes through the vehicle and is orthogonal to the position vector. It is the y-z plane in the rotating coordinate frame. The flight path angle, γ, is defined as the angle from the local horizontal plane to the velocity vector, $\vec{v}$. This angle is positive when measured above the local horizontal plane. The heading angle, ψ, is the angle from the local meridian of longitude to the projection of $\vec{v}$ on the local horizontal plane. This angle is positive when measured eastward. Figures 2-1 through 2-3 show the coordinate systems and the various quantities described above.

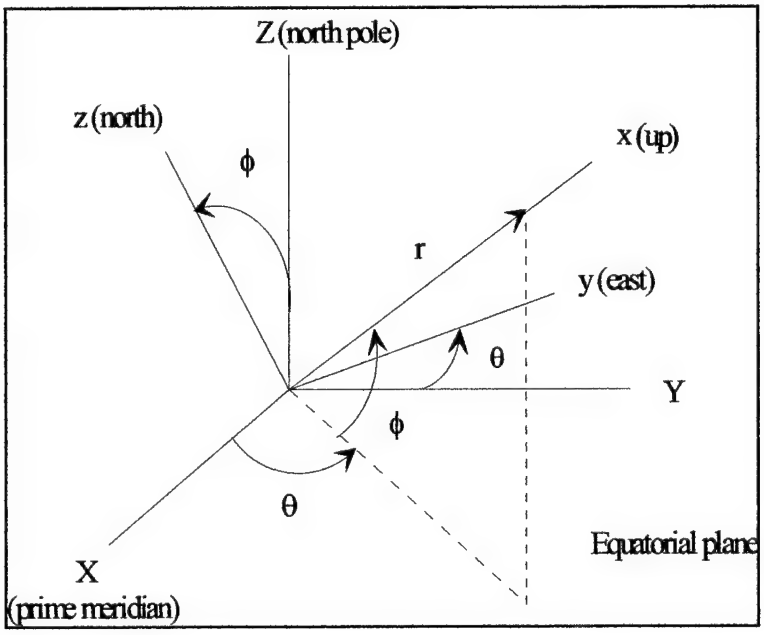

Figure 2-1. Reference Frames

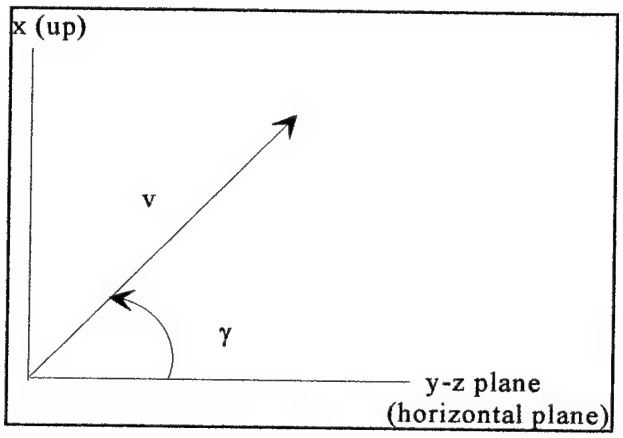

Figure 2-2. Flight path Angle

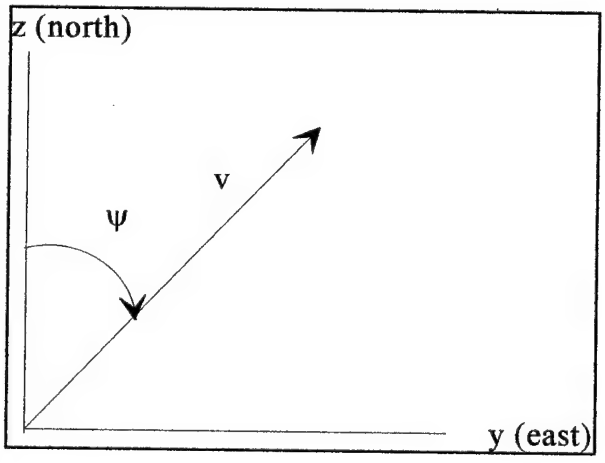

Figure 2-3. Heading Angle

2.3 State Variables and Equations of Motion

Now that the reference frames are defined, the problem can be set up. First, I'll define the variables of interest for the state space vector. These 7 elements are:

r – magnitude of the radius vector
θ - longitude of the vehicle
ϕ - latitude of the vehicle
v – speed of the vehicle
γ - flight path angle
ψ - heading
m – mass of the vehicle

Note that this is a traditional six-element state vector but mass is carried along with the state since this will be one of the important elements to examine for the trajectories that will be flown.

We are now ready to start developing equations of motion. The equation we need to determine the various components for is the five-part acceleration form of Newton's Second Law for a rotating frame:

$$m\frac{d\vec{v}}{dt} = \vec{F} - 2m\vec{\omega}\times\vec{v} - m\vec{\omega}\times(\vec{\omega}\times\vec{r}) \tag{2-1}$$

Let $\hat{i}$, $\hat{j}$, $\hat{k}$ define unit vectors in the x,y,z rotating frame. Developing the right-hand side first, we can write directly from the diagrams,

$$\vec{r} = r\,\hat{i} \tag{2-2}$$

and,

$$\vec{v} = (v\sin\gamma)\,\hat{i} + (v\cos\gamma\sin\psi)\,\hat{j} + (v\cos\gamma\cos\psi)\,\hat{k} \tag{2-3}$$

Writing $\vec{\omega}$ in terms of the rotating frame (x,y,z) gives,

$$\vec{\omega} = (\omega\sin\phi)\,\hat{i} + (\omega\cos\phi)\,\hat{k} \tag{2-4}$$

We can now write:

$$\vec{\omega}\times\vec{v} = -(\omega v\cos\phi\cos\gamma\sin\psi)\,\hat{i} + (\omega v(\cos\phi\sin\gamma - \sin\phi\cos\gamma\cos\psi))\,\hat{j} + (\omega v\sin\phi\cos\gamma\sin\psi)\,\hat{k}$$

and,

$$\vec{\omega}\times(\vec{\omega}\times\vec{r}) = -(r\omega^2\cos^2\phi)\,\hat{i} + (r\omega^2\sin\phi\cos\phi)\,\hat{k}$$

The final term on the right-hand side of (2-1) is $\vec{F}$, the force term. The forces acting on the vehicle are gravity, the aerodynamic forces, lift, $\vec{L}$ and drag, $\vec{D}$, and the propulsive force thrust, $\vec{T}$. The drag force, $\vec{D}$, is defined to be opposite to the velocity vector $\vec{v}$, and the lift force, $\vec{L}$, is orthogonal to it. We assume symmetric flight for this vehicle such that $\vec{T}$ occurs in the lift-drag plane. We define angle of attack, α, as the angle between $\vec{T}$ and $\vec{v}$. This allows us to write the components of thrust along the lift and velocity vectors as $T\sin\alpha$ and $T\cos\alpha$ respectively. It is now convenient to group the aerodynamic and propulsive force components together. Let F_T be the component along the velocity vector and F_N be the component orthogonal to F_T such that:

$$\begin{aligned} F_T &= T\cos\alpha - D \\ F_N &= T\sin\alpha + L \end{aligned} \tag{2-5}$$

We can now define the force vectors in the rotating frame (x,y,z). The force due to gravity can be written as:

$$\vec{F}_g = m\vec{g} = -mg(r)\,\hat{i} \tag{2-6}$$

In addition, since $\vec{F}_T$ is oriented along $\vec{v}$, we can write from equation 2-2:

$$\vec{F}_T = (F_T\sin\gamma)\,\hat{i} + (F_T\cos\gamma\sin\psi)\,\hat{j} + (F_T\cos\gamma\cos\psi)\,\hat{k} \tag{2-7}$$

The final force vector to be written is $\vec{F}_N$, which is the force collinear with lift. Lift is in the $\vec{r},\vec{v}$ (vertical) plane when the vehicle is in planar flight. Roll, σ, is the angle the lift vector makes with the vertical plane and is measured positive to the right. We can now decompose $\vec{F}_N$ into components $F_N\cos\sigma$ along the vertical plane (orthogonal to $\vec{v}$) and $F_N\sin\sigma$ orthogonal to the vertical plane. This now forms a right-handed system (a, b, c) = $(\overrightarrow{F_N\cos\sigma},\vec{v},\overrightarrow{-F_N\sin\sigma})$. Our rotating frame (x,y,z), can be obtained from (a,b,c) by a rotation ψ of the horizontal plane and a rotation γ of the vertical plane such that:

$$\begin{bmatrix} i \\ j \\ k \end{bmatrix} = \begin{bmatrix} 1 & 0 & 0 \\ 0 & \sin\psi & -\cos\psi \\ 0 & \cos\psi & \sin\psi \end{bmatrix} \begin{bmatrix} \cos\gamma & \sin\gamma & 0 \\ -\sin\gamma & \cos\gamma & 0 \\ 0 & 0 & 1 \end{bmatrix} \begin{bmatrix} a \\ b \\ c \end{bmatrix}$$

This allows us to write $\vec{F}_N = (F_N\cos\sigma)\,\hat{a} - (F_N\sin\sigma)\,\hat{c}$ in the rotating frame as:

$$\vec{F}_N = \begin{pmatrix} F_N\cos\sigma\cos\gamma \\ F_N(\sin\sigma\cos\psi - \cos\sigma\sin\gamma\sin\psi) \\ -F_N(\cos\sigma\sin\gamma\cos\psi - \sin\sigma\sin\psi) \end{pmatrix}^T \begin{pmatrix} \hat{i} \\ \hat{j} \\ \hat{k} \end{pmatrix} \qquad (2\text{-}8)$$

We now have all of the pieces for the right-hand side of equation 2-1 decomposed into components in the (x,y,z) rotating frame. In order to obtain the left-hand side of equation 2-1, we need to take derivatives, in the planet frame, of equation 2-2. In order to do so, we must determine how the (x,y,z) frame is rotating with respect to the planet frame. Recall that the (x,y,z) frame is derived by a rotation in θ about the Z-axis of the planetary frame followed by a rotation in ϕ about the negative y-axis of the rotating frame. Also

recalling the transformation between the frames used for equation 2-4, we can write the rotation of the (x,y,z) frame with respect to the (X,Y,Z) frame as:

$$\vec{\Omega} = (\dot{\theta}\sin\phi)\,\hat{i} - (\dot{\phi})\,\hat{j} + (\dot{\theta}\cos\phi)\,\hat{k}$$

The derivative with respect to the planetary frame of equation 2-2, $\frac{{}^{P}d\vec{r}}{dt}$, can now be calculated as:

$$\vec{v} = \frac{{}^{P}d\vec{r}}{dt} = \frac{d\vec{r}}{dt} + \vec{\Omega}\times\vec{r} = (\dot{r})\,\hat{i} + (r\dot{\theta}\cos\phi)\,\hat{j} + (r\dot{\phi})\,\hat{k} \qquad (2\text{-}9)$$

Equating components of equations 2-3 and 2-9 yields the first three scalar equations of motion:

$$\begin{aligned} \dot{r} &= v\sin\gamma \\ \dot{\theta} &= \frac{v\cos\gamma\sin\psi}{r\cos\phi} \\ \dot{\phi} &= \frac{v\cos\gamma\cos\psi}{r} \end{aligned} \qquad (2\text{-}10)$$

Next, we take the inertial derivative of 2-9 to obtain the appropriate components for the left-hand side of equation 2-1. Grouping the equations for the right-hand side of 2-1 by component and setting them equal to the components of the derivative of equation 2-9 yields a complicated version of the other three scalar equations of motion. Some tedious (and sometimes tricky) algebraic manipulation coupled with substitutions from equations 2-10 is required to get these equations in a more useful and reduced form. In addition, ω^2 terms are dropped from the derivation since ω, the rotation of the earth, is small on the

time-scale of this problem. The results of this effort yields the following set of scalar equations:

$$\begin{aligned}
\dot{v} &= \frac{1}{m}F_T - g\sin\gamma \\
v\dot{\gamma} &= \frac{1}{m}F_N\cos\sigma - g\cos\gamma + \frac{v^2}{r}\cos\gamma + 2\omega v\cos\phi\sin\psi \\
v\dot{\psi} &= \frac{F_N\sin\sigma}{m\cos\gamma} + \frac{v^2}{r}\cos\gamma\sin\psi\tan\phi + 2\omega v(\sin\phi - \cos\phi\cos\psi\tan\gamma)
\end{aligned} \tag{2-11}$$

Before we can replace F_T and F_N in equation 2-11 with the equations derived in 2-5, we need to define the lift and drag terms, L and D, explicitly. These equations are:

$$\begin{aligned}
L &= \frac{1}{2}c_L S\rho v^2 \\
D &= \frac{1}{2}c_D S\rho v^2
\end{aligned} \tag{2-12}$$

where c_D and c_L are the coefficients of drag and lift respectively, S is the surface area of the vehicle, and ρ is the atmospheric density. Substituting 2-12 into equation 2-5 gives:

$$\begin{aligned}
F_T &= T\cos\alpha - \frac{1}{2}c_D S\rho v^2 \\
F_N &= T\sin\alpha + \frac{1}{2}c_L S\rho v^2
\end{aligned} \tag{2-13}$$

We define the mass flow rate as:

$$\dot{m} = \beta = -\frac{T}{g_0 I_{sp}} \tag{2-14}$$

where T is thrust, g_0 is acceleration due to gravity at sea level, and I_{sp} is specific impulse.

Making the final substitution of 2-13 into 2-11, recalling equation 2-10, and adding 2-14 gives the seven scalar equations of motion for this system:

$$
\begin{aligned}
\dot{r} &= v\sin\gamma \\
\dot{\theta} &= \frac{v\cos\gamma\sin\psi}{r\cos\phi} \\
\dot{\phi} &= \frac{v\cos\gamma\cos\psi}{r} \\
\dot{v} &= \frac{T\cos\alpha}{m} - \frac{c_D S\rho v^2}{2m} - g\sin\gamma \\
\dot{\gamma} &= \frac{T\sin\alpha\cos\sigma}{mv} + \frac{c_L S\rho v\cos\sigma}{2m} - \frac{g\cos\gamma}{v} + \frac{v\cos\gamma}{r} + 2\omega\cos\phi\sin\psi \\
\dot{\psi} &= \frac{T\sin\alpha\sin\sigma}{mv\cos\gamma} + \frac{c_L S\rho v\sin\sigma}{2m\cos\gamma} + \frac{v\cos\gamma\sin\psi\tan\phi}{r} + 2\omega(\sin\phi - \cos\phi\cos\psi\tan\gamma) \\
\dot{m} &= \beta = -\frac{T}{g_0 I_{sp}}
\end{aligned}
\tag{2-15}
$$

The traditional form for equations of motion for a non-linear time-dependent system is:

$$\dot{x} = f(x, u, t) \tag{2-16}$$

where x represents the state variables, and u represents the control variables. That tradition will be continued here as 2-16 is a more convenient form for further discussions. Now that the equations of motion are defined, we are ready to bring optimal control into the discussion, which will begin, in chapter three.

III. OPTIMAL CONTROL

3.1 Introduction

This chapter is devoted to the development and discussion of optimal control methods presented in Bryson and Ho [2, 87-89], and their utilization in the solution of this problem. Specifically, we will look at optimizing a continuous, dynamic system with functions of the state variables specified at an unknown final time. The objective is to solve a minimum time launch to rendezvous scenario by determining the initial state and co-state values that will satisfy a desired set of final conditions. A boundary value problem will be posed which will establish these constrained final conditions. The result will determine a solution trajectory, given in terms of the state variables, and a final time which are optimal.

3.2 Optimal Control Development

We begin by defining the performance index, which we want to minimize:

$$J = \phi[x(t_f), t_f] + \int_{t_0}^{t_f} L[x(t), u(t), t]dt \tag{3-1}$$

where $\phi[x(t_f), t_f]$ defines the final boundary conditions as a function of the state at the final time and the final time, and $L[x(t), u(t), t]$ is a Lagrangian function that is a function of the state, $x(t)$, the control vector, $u(t)$, and time. Next, we define a vector function, ψ, which defines the constraints at the final time such that

$$\psi[x(t_f), t_f] = 0. \tag{3-2}$$

We want to adjoin the constraints from 3-2 and the differential equations of motion

$$\dot{x} = f[x(t), u(t), t], \qquad t_0 \text{ given} \tag{3-3}$$

to 3-1 with Lagrange multipliers ν and $\lambda(t)$ respectively. Making these substitutions results in the following equation:

$$J = [\phi + \nu^T \psi]_{t=t_f} + \int_{t_0}^{t_f} \{L(x,u,t) + \lambda^T [f(x,u,t) - \dot{x}]\} dt. \tag{3-4}$$

We can now define the Hamiltonian function as

$$H = L(x,u,t) + \lambda^T(t) f(x,u,t) \tag{3-5}$$

and make the following substitution

$$\Phi = \phi + \nu^T \psi. \tag{3-6}$$

Substituting 3-5 and 3-6 into 3-4 and taking the differential yields

$$dJ = \left(\left(\frac{\partial \Phi}{\partial t} + L \right) dt + \frac{\partial \Phi}{\partial x} dx \right)_{t=t_f} + \int_{t_0}^{t_f} \left(\frac{\partial H}{\partial x} \delta x + \frac{\partial H}{\partial u} \delta u - \lambda^T \delta \dot{x} \right) dt - L \big|_{t=t_0} dt_0. \tag{3-7}$$

The next step is to integrate 3-7 by parts to get

$$\begin{aligned} dJ = &\left(\frac{\partial \Phi}{\partial t} + L + \lambda^T \dot{x} \right)_{t=t_f} dt_f + \left[\left(\frac{\partial \Phi}{\partial x} - \lambda^T \right) dx \right]_{t=t_f} + (\lambda^T \delta x)_{t=t_0} \\ &+ \int_{t_0}^{t_f} \left[\left(\frac{\partial H}{\partial x} + \dot{\lambda}^T \right) \delta x + \frac{\partial H}{\partial u} \delta u \right] dt - L \big|_{t=t_0} dt_0. \end{aligned} \tag{3-8}$$

Since t_f is unspecified, we want to choose the $\lambda(t)$ to make the coefficients of $\delta x(t)$, $dx(t_f)$, and dt_f in equation 3-8, equal to zero. In other words, we want:

$$\dot{\lambda}^T = -\frac{\partial H}{\partial x} = -\lambda^T \frac{\partial f}{\partial x} - \frac{\partial L}{\partial x}, \tag{3–9}$$

$$\lambda^T(t_f) = \left(\frac{\partial \Phi}{\partial x} \right)_{t=t_f} = \left(\frac{\partial \phi}{\partial x} + \nu^T \frac{\partial \psi}{\partial x} \right)_{t=t_f}, \text{ and} \tag{3–10}$$

$$\left(\frac{\partial \Phi}{\partial t} + L + \lambda^T \dot{x} \right)_{t=t_f} = \left(\frac{\partial \Phi}{\partial t} + \frac{\partial \Phi}{\partial x} \dot{x} + L \right)_{t=t_f} = 0 \tag{3–11}$$

As a result of imposing these conditions, 3-8 can now be simplified to the following form:

$$dJ = \lambda^T(t_0)dx(t_0) + \int_{t_0}^{t_f} \frac{\partial H}{\partial u}\delta u dt - H(t_0)dt_0 . \qquad (3\text{-}12)$$

From equation 3-12, we can conclude that changes in J will occur if: at t_0, unspecified state variables have non-zero corresponding Lagrange multipliers, or $\frac{\partial H}{\partial u}$ is non-zero as the result of unit impulses in the controls on the interval $t_0 \le t \le t_f$, or t_0 is unspecified, which is not the case here. Since we are trying to extremize J, we want $dJ = 0$, and therefore, we can write:

$$\frac{\partial H}{\partial u} = \lambda^T \frac{\partial f}{\partial u} + \frac{\partial L}{\partial u} = 0, \qquad t_0 \le t \le t_f . \qquad (3\text{-}13)$$

We can also make the statement that any state variable which is free to vary (unspecified) at $t = t_0$, $x_i(t_0)$, will have its corresponding Lagrange multiplier equal to zero, $\lambda_i(t_0) = 0$. We can now write all of the equations necessary for a stationary value of J as:

$$\dot{x} = f(x,u,t), \qquad (3\text{-}14)$$

$$\dot{\lambda} = -\frac{\partial H}{\partial x} = -\lambda^T \frac{\partial f}{\partial x} - \frac{\partial L}{\partial x}, \qquad (3\text{-}15)$$

$$0 = \frac{\partial H}{\partial u} = \lambda^T \frac{\partial f}{\partial u} + \frac{\partial L}{\partial u}, \qquad (3\text{-}16)$$

$$x_i(t_0) \quad \text{specified,} \quad \text{or} \quad \lambda_i(t_0) = 0 , \qquad (3\text{-}17)$$

$$\lambda(t_f) = \left(\frac{\partial \phi}{\partial x} + \nu^T \frac{\partial \psi}{\partial x}\right)^T_{t=t_f}, \qquad (3\text{-}18)$$

$$\Omega = \left[\frac{\partial \phi}{\partial t} + \nu^T \frac{\partial \psi}{\partial t} + \left(\frac{\partial \phi}{\partial x} + \nu^T \frac{\partial \psi}{\partial x}\right) f + L\right]_{t=t_f} = 0, \qquad (3\text{-}19)$$

$$\psi[x(t_f), t_f] = 0 . \qquad (3\text{-}20)$$

3.3 Application of Optimal Control

Now that we know the equations we need to solve this problem, equations 3-14 through 3-20, we need to write these equations in terms of the variables and conditions of this problem. Since this is a minimum time problem, we can state that $\phi[x(t_f),t_f] = 0$ and $L = 1$. This is a standard method for minimum time optimization and will not be derived here. We're not going to rewrite the equations of the previous section to reflect these conditions, however these substitutions will be made in the development of the equations henceforth.

We begin by recognizing that we already know the first equation, 3-14 as the set of seven, scalar equations of motion 2-15. This allows us to proceed to writing equation 3-15. In order to do this, we first define the Lagrange multipliers, $\lambda(t)$, as:

$$\lambda^T(t) = \left(\lambda_r, \lambda_\theta, \lambda_\phi, \lambda_v, \lambda_\gamma, \lambda_\psi, \lambda_m\right). \tag{3-21}$$

Note that the subscripts match the state variables and thus they are sometimes referred to as the co-state variables. We can now define the Hamiltonian function from 3-5, as $H(t) = L(x,u,t) + \lambda^T(t) f(x,u,t)$. Expanding this out gives:

$$H(t) = 1 + \left\{ \begin{array}{l} \lambda_r(v\sin\gamma) + \lambda_\theta\left(\dfrac{v\cos\gamma\sin\psi}{r\cos\phi}\right) + \lambda_\phi\left(\dfrac{v\cos\gamma\cos\psi}{r}\right) \\ +\lambda_v\left(\dfrac{T\cos\alpha}{m} - \dfrac{c_D S\rho v^2}{2m} - g\sin\gamma\right) \\ +\lambda_\gamma\left(\dfrac{T\sin\alpha\cos\sigma}{mv} + \dfrac{c_L S\rho v\cos\sigma}{2m} - \dfrac{g\cos\gamma}{v} + \dfrac{v\cos\gamma}{r} + 2\omega\cos\phi\sin\psi\right) \\ +\lambda_\psi\left(\dfrac{T\sin\alpha\sin\sigma}{mv\cos\gamma} + \dfrac{c_L S\rho v\sin\sigma}{2m\cos\gamma} + \dfrac{v\cos\gamma\sin\psi\tan\phi}{r} + 2\omega(\sin\phi - \cos\phi\cos\psi\tan\gamma)\right) \\ +\lambda_m\beta \end{array} \right\} \tag{3-22}$$

Taking the partial derivatives of equation 3-22 with respect to each of the seven state variables, will yield seven more scalar equations. These equations are termed the co-state equations of motion, as they describe how the co-state variables are changing with time. These equations are very long and are presented in Appendix A.

Next, we want to determine the appropriate equations from 3-16. Taking the partial derivatives of 3-22 with respect to the control variables, roll (σ) and angle of attack (α), will give two equations, equal to zero, termed the optimality conditions. These equations can then be solved for the respective control variable to yield the control laws. Taking $\frac{\partial H}{\partial \sigma}$ gives the first optimality condition:

$$-\lambda_\gamma\left(\frac{T\sin\alpha\sin\sigma}{mv}+\frac{c_L S\rho v\sin\sigma}{2m}\right)+\lambda_\psi\left(\frac{T\sin\alpha\cos\sigma}{mv\cos\gamma}+\frac{c_L S\rho v\cos\sigma}{2m\cos\gamma}\right)=0. \qquad (3\text{-}23)$$

Solving 3-23 for σ, yields the control law for roll:

$$\sigma = \tan^{-1}\left(\frac{\lambda_\psi}{\lambda_\gamma}\sec\gamma\right). \qquad (3\text{-}24)$$

Taking $\frac{\partial H}{\partial \alpha}$ yields the second optimality condition, given by:

$$-\lambda_v\left(\frac{T\sin\alpha}{m}+\frac{c_D' S\rho v^2}{2m}\right)+\lambda_\gamma\left(\frac{T\cos\alpha\cos\sigma}{mv}+\frac{c_L' S\rho v\cos\sigma}{2m}\right)+\lambda_\psi\left(\frac{T\cos\alpha\sin\sigma}{mv\cos\gamma}+\frac{c_L' S\rho v\sin\sigma}{2m\cos\gamma}\right)=0 \qquad (3\text{-}25)$$

where c_D' and c_L' are the derivatives with respect to α. These terms appear because c_D and c_L are both functions of the angle of attack. Equation 3-25 cannot be solved explicitly for α because of this dependence. We can, however, make a good approximation for α if we assume that the aerodynamic forces are much smaller than the

thrust terms and can thus be neglected. This is reasonable because the scenarios considered in this research either had no atmosphere or applied the optimal control outside of the atmosphere. Using this assumption, equation 3-25 reduces to:

$$-\lambda_v\left(\frac{T\sin\alpha}{m}\right)+\lambda_\gamma\left(\frac{T\cos\alpha\cos\sigma}{mv}\right)+\lambda_\psi\left(\frac{T\cos\alpha\sin\sigma}{mv\cos\gamma}\right)=0 \tag{3-26}$$

which can be solved for α to yield the approximate control law for angle of attack:

$$\alpha \approx \tan^{-1}\left(\frac{1}{\lambda_v v}\left(\lambda_\gamma \cos\sigma + \lambda_\psi \sec\gamma \sin\sigma\right)\right). \tag{3-27}$$

Now that we have the control laws defined, we can move on to condition 3-17 to help determine the initial conditions of the state and co-state variables.

At the initial time, $t = t_0$, the state and co-state variables will either be specified, free to vary, or zero. We can specify all of the state variables at the initial time except the flight path angle, γ, and the heading, ψ which are both free to vary. From condition 3-17, this implies that λ_γ and λ_ψ must be equal to zero at t_0. The rest of the co-state variables are free to vary at t_0. So, we can write the state and co-state variables at $t = t_0$ as:

$$x(t_0)=\begin{bmatrix} r-\text{specified} \\ \theta-\text{specified} \\ \phi-\text{specified} \\ v-\text{specified} \\ \gamma-\text{free} \\ \psi-\text{free} \\ m-\text{specified} \end{bmatrix} \qquad \lambda(t_0)=\begin{bmatrix} \lambda_r-\text{free} \\ \lambda_\theta-\text{free} \\ \lambda_\phi-\text{free} \\ \lambda_v-\text{free} \\ \lambda_\gamma=0 \\ \lambda_\psi=0 \\ \lambda_m-\text{specified}=0 \end{bmatrix} \tag{3-28}$$

Since we are carrying the mass, m, in the state for convenience, not necessity, λ_m is carried for symmetry. It does not influence the equations of motion or the control laws that have been derived, so we can ignore it. Therefore, its value will be specified at zero

on the entire interval $t_0 \leq t \leq t_f$. The remainder of the specified values will be determined based on the choice for t_0. The final step is to complete the boundary value problem, and establish the requirements for the vehicle at time $t = t_f$, including determining t_f.

We will use equations 3-18 through 3-20 for this process. We begin by noting that there are a total of seven free initial conditions, six shown in 3-28 and the final time t_f. Since we're trying to find the minimum time trajectory, t_f can be thought of as a free initial condition. Having seven free initial conditions dictates that we must have seven boundary conditions at the final time. We can conclude that we need to specify an altitude, a speed, the vehicle flying level, a heading, and ensure the vehicle is in the proper orbital plane. This gives five conditions, which means we'll have to use 3-18 and 3-19 to specify the other two conditions.

The first condition we want to specify is that the altitude at the final time is equal to the altitude of the low earth orbit we are trying to reach, r_f. Therefore, we require:

$$r(t_f) = r_f . \tag{3-29}$$

The second condition we will specify is that the vehicle is traveling level or in the horizontal plane at t_f. This stipulates that:

$$\gamma(t_f) = 0 . \tag{3-30}$$

The third condition is to specify that the speed of the vehicle has reached orbital speed, which is ≈ 7.5 km/s in low earth orbit. It is important to note that this speed is with respect to the inertial, earth centered frame. Up to this point, the speed, v, has been defined with respect to the rotating frame (x,y,z). Therefore we must define the speed to

include the component due to the earth's rotation. The velocity with respect to the inertial frame can be written as:

$$\overrightarrow{v_I} = \vec{v} + \vec{\omega} \times \vec{r}$$

Since we specified $\gamma = 0$ above, we can refer back to Figure 2-3 and modify equation 2-3 to state the inertial velocity at t_f is:

$$\overrightarrow{v_I} = (v \sin\psi + \omega r \cos\phi)\,\hat{j} + (v \cos\psi)\,\hat{k}. \tag{3-31}$$

Taking the magnitude of 3-31, gives the inertial speed we desire:

$$v_I = \left[(v \sin\psi + \omega r \cos\phi)^2 + v^2 \cos^2\psi\right]^{\frac{1}{2}} \tag{3-32}$$

The third condition for orbital speed can now be written as:

$$v_I(t_f) = v_f \tag{3-33}$$

The next two conditions require some spherical trigonometry. The fourth condition requires that the vehicle have the proper heading at the final time. Like the speed, this heading is with respect to the inertial frame. As a result of adding the rotation of the earth component to the velocity (3-31), we now must define the inertial heading, ψ_I, as:

$$\psi_I = \tan^{-1}\left(\frac{v \sin\psi + \omega r \cos\phi}{v \cos\psi}\right) \tag{3-34}$$

Consider the diagram in Figure 3-1. We know i, the inclination, θ, the final longitude, and ϕ, the final latitude of the orbit we're trying to achieve. In order to have the correct heading, we must specify ψ_I at t_f such that:

$$\cos\psi_I = \cos(\theta - \theta_{orb})\sin(i). \tag{3-35}$$

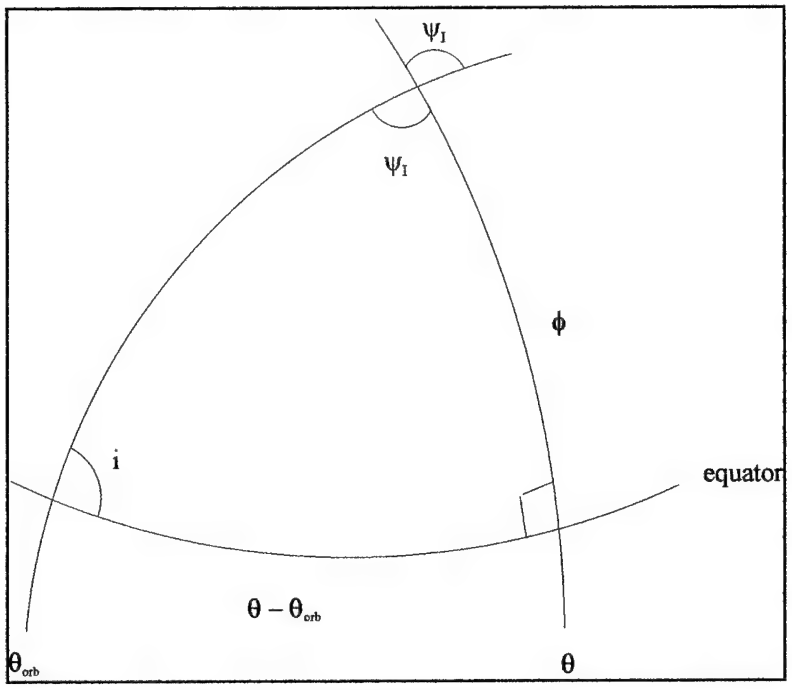

Figure 3-1 Determining Heading and Plane Conditions

For the fifth condition, we want to specify that the vehicle is in the desired orbital plane. Referring to Figure 3-1 again, we can define the plane condition by mandating θ_{orb} such that:

$$\sin(\theta - \theta_{orb}) = \tan\phi \mathrm{ctn}(i). \tag{3-36}$$

We can now use equations 3-29 through 3-36 along with condition 3-20 to define five of the boundary conditions as:

$$\psi[x(t_f), t_f] = \begin{bmatrix} r - r_f \\ v_I - v_f \\ \gamma \\ \cos\psi_I - \cos(\theta - \theta_{orb})\tan(i) \\ \sin(\theta - \theta_{orb}) = \tan\phi \mathrm{ctn}(i) \end{bmatrix} = \begin{bmatrix} 0 \\ 0 \\ 0 \\ 0 \\ 0 \end{bmatrix} \tag{3-37}$$

Now we will derive the other two final conditions. Substituting $\phi[x(t_f),t_f] = 0$, L = 1, and 3-18 into 3-19 and noticing 3-32 has no explicit time dependence, 3-19 reduces to:

$$\Omega = \left(\lambda^T f + L\right)_{t=t_f} = 0$$

Referring to equation 3-5, this is the Hamiltonian at $t = t_f$. Therefore our sixth boundary condition is:

$$H(t_f) = 0. \tag{3-38}$$

Equation 3-38 determines the value for the final time.

The quest for the final boundary condition will now commence. We start by recalling and expanding equation 3-6, also making the appropriate substitution for $\phi[x(t_f),t_f]$ to yield the following result:

$$\Phi(t_f) = \left(\nu^T \psi\right)_{t=t_f} = \begin{bmatrix} \nu_1(r - r_f) \\ \nu_2(v_I - v_f) \\ \nu_3 \gamma \\ \nu_4\left(\cos\psi_I - \cos(\theta - \theta_{orb})\sin(i)\right) \\ \nu_5\left(\sin(\theta - \theta_{orb}) - \tan\phi \text{ctn}(i)\right) \end{bmatrix} \tag{3-39}$$

At this point, we refer back to equation 3-18 and take the partial derivative of 3-39 with respect to the state variables to determine $\lambda(t_f)$. Doing this yields

$$\lambda(t_f) = \begin{bmatrix} \lambda_r \\ \lambda_\theta \\ \lambda_\phi \\ \lambda_v \\ \lambda_\gamma \\ \lambda_\psi \\ \lambda_m \end{bmatrix}_{t=t_f} = \begin{bmatrix} \nu_1 + \nu_2 A - \nu_4 B \\ \nu_4 \sin(\theta - \theta_{orb})\sin(i) + \nu_5 \cos(\theta - \theta_{orb}) \\ -\nu_2 C + \nu 4 D - \nu_5 \sec^2 \phi \text{ctn}(i) \\ \nu_2 E + \nu_4 F \\ \nu_3 \\ \nu_2 G - \nu_4 I \\ 0 \end{bmatrix}_{t=t_f} \tag{3-40}$$

where the following simplifications have been made:

$$A = \frac{\omega \cos\phi(v \sin\psi + \omega r \cos\phi)}{v_I} \tag{3-41}$$

$$B = \frac{\sin\psi_I \omega v \cos\phi \cos\psi}{v_I^2} \tag{3-42}$$

$$C = \frac{\omega r \sin\phi(v \sin\psi + \omega r \cos\phi)}{v_I} \tag{3-43}$$

$$D = \frac{\sin\psi_I \omega r v \sin\phi \cos\psi}{v_I^2} \tag{3-44}$$

$$E = \frac{v + \omega r \cos\phi \sin\psi}{v_I} \tag{3-45}$$

$$F = \frac{\sin\psi_I(\cos\psi(v \sin\psi + \omega r \cos\phi) - v \cos\psi \sin\psi)}{v_I^2} \tag{3-46}$$

$$G = \frac{\omega r \cos\phi \cos\psi}{v_I} \tag{3-47}$$

$$I = \frac{\sin\psi_I(v^2 - \omega r v \cos\phi \sin\psi)}{v_I^2}. \tag{3-48}$$

There are two items of interest to mention at this point. First notice that in equation 3-40, $\lambda_m = 0$ by calculation. This further reinforces the decision to ignore it. Second, there are six remaining equations in 3-40, and five unknown multipliers, ν. This is the key to boundary condition number seven. Using the third, fourth, and sixth equations to solve for ν_2, ν_4, and ν_5 and substituting the results into the second equation gives the following equation which is independent of the unknown ν's:

$$\left[\lambda_{\cdot\theta} + \left(\frac{\lambda_\psi E + \lambda_v G}{(IE + FG)}\right)\sin(\theta - \theta_{orb})\sin(i) + \left(\frac{\lambda_\phi(IE + FG) + \lambda_\psi(ED + CF) + \lambda_v(IC - DG)}{(IE + FG)\sec^2\phi \operatorname{ctn}(i)}\right)\cos(\theta - \theta_{orb})\right] = 0 \tag{3-49}$$

Equation 3-49 is the seventh boundary condition. Now, let's summarize the results from all of this derivation. Pulling together 3-37, 3-38, and 3-49 gives the seven boundary conditions at $t = t_f$ as

$$\psi[x(t_f),t_f]=\begin{bmatrix} r-r_f \\ v_I-v_f \\ \gamma \\ \cos\psi_I-\cos(\theta-\theta_{orb})\sin(i) \\ \sin(\theta-\theta_{orb})-\mathrm{ctn}(i)\tan\phi \\ H \\ \lambda_\theta+\left(\dfrac{\lambda_\psi E+\lambda_v G}{(IE+FG)}\right)\sin(\theta-\theta_{orb})\sin(i) \\ +\left(\dfrac{\lambda_\phi(IE+FG)+\lambda_\psi(ED+CF)+\lambda_v(IC-DG)}{(IE+FG)\sec^2\phi\,\mathrm{ctn}(i)}\right)\cos(\theta-\theta_{orb}) \end{bmatrix}=\begin{bmatrix}0\\0\\0\\0\\0\\0\\0\end{bmatrix} \quad (3\text{-}50)$$

Now we have the boundary conditions at the final time, and we've identified which of the variables are specified, zero, or free to vary at the initial time, (3-28). The boundary value problem is set up and the next step is to specify the initial and final numerical values necessary, and start integrating trajectories. These trajectories will all be optimal, but probably will not leave us where we want. But, by making small corrections to the free initial conditions we can slowly 'step' to the coplanar solution we want. Once we have that, we can make changes to extrapolate away from the coplanar solution to the non-coplanar solutions. The algorithms developed to do this will be discussed in the next chapter.

IV. ALGORITHMS

4.1 Introduction

To this point, the theoretical development of this problem has been presented. Now, the algorithms developed to model the problem will be discussed. Before we get into the details though, a few assumptions must be listed.

1. Aerodynamics have been neglected, i.e. $c_D = c_L = 0$.
2. Engine throttling capability exists for the vehicle.
3. Loaded weight of the vehicle is 1,279,000 lbs. (= 580,145.5153 kg)
4. Dry weight for the vehicle is 104,100 lbs. (= 47,219.03686 kg).
5. The derivations and assumptions of the previous chapters are accurate.

In addition to the assumptions, a standardized set of dimensionless units was defined in order to avoid conflicts with different unit systems. This unit system is defined as follows:

Distance Unit: 1 DU = 6378145 m.

Mass Unit: 1 MU = 5.976×10^{24} kg.

Time Unit: 1 TU = 806.8118744 sec.

Using these assumptions along with the equations of motion and the seven final boundary conditions, three computer algorithms have been developed to model the launch trajectories of the vehicle. The first program, LAUNCH, integrates a launch trajectory to a guessed final time and compares the end conditions to those we have specified from equation 3-50. Corrections are then made to the free variables at the initial time (refer to equation 3-28) and a new trajectory is integrated. This process

continues until the initial conditions are determined which satisfy the final conditions. These initial conditions give the solution for the coplanar trajectory. Once the initial coplanar solution is known, the second program, EXTRAPI, is used to find coplanar solutions for different orbit inclinations. The result is a list of converged initial conditions for each inclination that was specified. The third program, EXTRAP, is used to 'step' away from the coplanar solution to non-coplanar solutions by changing the longitude of the ascending node, θ_{orb}. The same iterative, convergence process is used to give the initial conditions for the non-coplanar trajectories over the specified range for θ_{orb}. A more detailed look at how these programs determine the solutions follows.

4.2 The Initial Coplanar Solution

As mentioned above, LAUNCH is used to find the initial coplanar solution for a given launch site and target orbit. The program begins by reading the following information from an input file:

- Initial 14-value state vector (the 7 state and 7 co-state variables are combined and now referred to as the state vector)
- Initial time, throttle time, and guess of final time
- Integration steps for the integrator
- Longitude of the ascending node and inclination for the target orbit
- An initial guess for the final conditions
- Amount to perturb reference trajectory (to be explained later)
- The desired values for the final conditions
- Number of steps used to go from the guessed trajectory to the desired one

After the input information is read in, the next step is to integrate a trajectory from the initial time to the throttle time and then again from the throttle time to the final time. The throttle time is the point where the vehicle is accelerating at approximately three g's. The thrust is then reduced by 50% and the integration is continued to the final time. This throttling is done to avoid large accelerations at burnout.

The subroutine HAMING is called to perform the numerical integration of the trajectory. HAMING is a fourth-order predictor-corrector algorithm, which uses the last four values of the state to predict the next value. The predicted value is then corrected using the equations of motion to obtain the new value of the state vector. This process continues for a specified duration determined by the number of integration steps and the final time. When HAMING is first initialized, we have only provided it with the first set of initial conditions, therefore, a Picard iteration is used to determine the next three values so that the predictor portion can begin. Once this is accomplished, the Picard iteration is no longer used and the predictor-corrector algorithm continues to the end time. HAMING calls a subroutine, RHS, which is the dynamics routine that contains the control laws, the equations of motion, and various values and conversions used in their determination.

Once the trajectory has been integrated, the values of the state vector at the final time, along with the orbit information from the input file, are used to evaluate the boundary conditions 3-50. We will call this vector ψ_{ref}. The vector ψ_{ref} is subtracted from the initial guess, ψ_0, to determine an error vector. The error vector tells us how far the reference trajectory is from our guess of the final boundary conditions.

The next step is to recognize that we can approximate ψ_0 in following form:

$$\psi_0 \approx \psi_{ref} + \frac{\partial \psi}{\partial x_{free}} \delta x_{free} \tag{4-1}$$

which can be rewritten as

$$\psi_0 - \psi_{ref} \approx \frac{\partial \psi}{\partial x_{free}} \delta x_{free} . \tag{4-2}$$

The error vector mentioned above is the left-hand side of equation 4-2, and δx_{free} gives the corrections to the free initial conditions that will give us $\psi_{ref} = \psi_0$. Therefore, we need to determine $\frac{\partial \psi}{\partial x_{free}}$. This is a 7 x 7 matrix that we will approximate by taking numerical partial derivatives. Each column of this matrix is determined by perturbing one of the free initial conditions by an amount δx, integrating the trajectory, and evaluating the final boundary conditions to get the vector ψ'. The i^{th} column of the matrix can be approximated by:

$$\left(\frac{\partial \psi}{\partial x_{free}} \right)_{col=i} \approx \frac{\psi_i' - \psi_{ref}}{\delta x_i} \tag{4-3}$$

Performing this seven times for each of the free initial conditions completes the matrix, which then allows us to solve the linear system in equation 4-2 for the vector δx_{free}. The subroutine LEQT2F does just this and gives us the corrections such that the new free initial conditions, $x_{free}(t_0)$, can be written as:

$$x_{free}(t_0) = x_{free}(t_0) + \delta x_{free} \tag{4-4}$$

This process iterates until the corrections to each free variable are below a predetermined value. At this point, the program has converged to a set of initial conditions which

produce the end conditions, ψ_0. Recall though that this is just the guess at final conditions, not the final conditions we desire. Therefore another loop is set up that changes the value of ψ_0 by an amount determined from the input file so that the trajectories 'step' toward the final desired trajectory. On the final iteration, ψ_0 is equal to our desired final conditions and the converged initial conditions provide the coplanar trajectory we were looking for. The convergence tolerance is relatively large during this process, and is narrowed once an initial coplanar solution is obtained in order to provide more accurate initial conditions. Once we have these initial conditions, we're ready to start extrapolating to different inclinations, and the non-coplanar solutions.

4.3 Extrapolating to Different Inclinations

Now that we have a solution for a given inclination, we can use it as a starting point to find the solutions for a range of different inclinations. For this research, the program LAUNCH was used to find the solution for a rendezvous orbit whose inclination was equal to the latitude of the launch site. From this solution, the inclination was increased in 0.5-degree intervals for a total of 31.5 degrees, and initial conditions were obtained for all 62 cases using the program EXTRAPI.

EXTRAPI works in much the same way as LAUNCH. The difference is that it changes the value of the inclination for each iteration rather than stepping the value of ψ_0. The guess for the final boundary conditions and the desired value for the boundary conditions are equal at this point from running LAUNCH. Instead, we modify the input file to give an initial inclination and a desired inclination along with the other quantities. For each new inclination determined, a new value of θ_{orb} is determined using the latitude

and longitude of the launch location, the new inclination, and equation 3-36. The new initial conditions are determined the same as in LAUNCH and are output to a separate file along with the inclination once convergence is achieved. The result is a database of initial conditions, which satisfy the coplanar boundary conditions for each specified inclination (28.5 – 60 degrees in 0.5-degree increments for this study).

4.4 Non-coplanar Solutions

The third program, EXTRAP, gives us the results that were the motivation for this research. The goal was to solve for non-coplanar launch trajectories and determine how much payload mass could be put in orbit by following them. EXTRAP takes the coplanar initial conditions for a given inclination, changes the longitude of the ascending node, θ_{orb}, by a specified amount, and converges to a new set of initial conditions using the same steps as LAUNCH. The input file differs from the EXTRAPI input file by specifying the range for θ_{orb} instead of for inclination. The range used for this study was +/- 11.25 degrees from the coplanar value for θ_{orb}. The orbital period for a low earth orbit is approximately 90 minutes. The ground trace for this orbit shifts approximately 22.5 degrees per orbit. Therefore, the worst case amount you would need to depart from the coplanar case would be half the range, or 11.25 degrees. When a set of initial conditions is converged upon for a given θ_{orb}, the mass at t_f is output to a separate file along with the value of θ_{orb}.

The results for the first of two scenarios are presented in the next chapter. This scenario depicts a situation in which the aerodynamics are non-existent. This was accomplished by setting the coefficients of lift and drag equal to zero. While this appears

to be an unrealistic scenario to consider, the results obtained give an optimistic look at payload masses that could be delivered to orbit on non-coplanar trajectories. Payload masses for several inclinations, as well as an analysis of the values of control variables along selected trajectories will be presented.

V. NON-AERODYNAMIC RESULTS

5.1 Introduction

As mentioned previously, this chapter presents the results for a non-aerodynamic scenario. The coefficients of lift and drag were set equal to zero throughout the trajectories in order to get an optimistic look at the payload mass deliverable to orbit as well as the control variables as a function of time. Five different rendezvous orbit cases were considered in this research. EXTRAPI was used to determine the free initial conditions for all but the first case, which were determined using LAUNCH. The first four cases examine non-coplanar trajectories off of the nominal coplanar solutions from this range. The inclinations selected for this study were, 28.5°, 35°, 45°, and 57°, which is near the inclination for the MIR space station. EXTRAP was then used to take the solutions for the coplanar case and extrapolate θ_{orb} plus 11.25° and minus 11.25°, in order to span the 22.5° range.

The coplanar initial conditions, the desired 11.25-degree range (plus or minus) for extrapolating θ_{orb}, and the other necessary input quantities described earlier were assembled for the input file to EXTRAP for each case. The algorithm broke the 11.25-degree range for θ_{orb} into 20 intervals and thus solved the initial conditions for 21 trajectories with the endpoints of the range included. When EXTRAP converged to a solution set of initial conditions for a particular θ_{orb}, the final mass of the vehicle, as well as the value of θ_{orb}, were output to a separate data file. The final mass was then converted to kilograms, and the dry mass of the vehicle (47,219 kg) subtracted. The resulting surplus was the payload mass that could be delivered to the specified orbit.

The final case considers launching into 25-degree inclination orbits from a launch latitude of 28.5-degrees. Again, EXTRAPI was used to determine the first set of initial conditions when the maximum latitude of the orbit occurred at the same longitude as the launch site. Then EXTRAP moved the orbit +/- 11.25-degrees and final masses were determined.

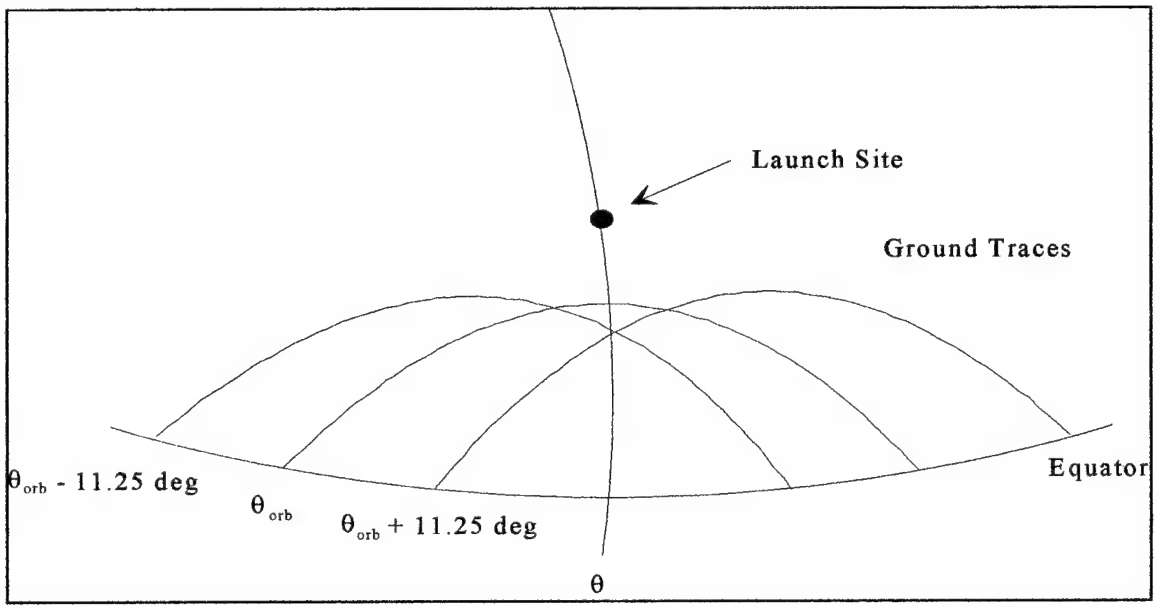

Figure 5-1. Case 5 Extrapolation

All of the cases used the same set of specified initial conditions, which are listed below in Table 5-1. R_{earth} in the table refers to the radius of the earth. These initial conditions were determined such that t_0 would occur 15 seconds after liftoff. This allowed the vehicle to clear any launch structure and perform any orientation maneuvering prior to the analysis of the trajectory. In addition, the final altitude and speed for the rendezvous orbit are listed in Table 5-2. These values were picked at random and do not have any special significance, other than defining a low earth orbit.

Table 5-1. Specified Initial Conditions

Altitude, $r - R_{earth}$	441 m
Longitude, θ	279.45 deg East
Latitude, ϕ	28.5 deg North
Speed, v	58.86 m/s
Mass, m	580,145.5153 kg
λ_γ	0
λ_ψ	0

Table 5-2. Specified Final Conditions

Altitude, r_f	220 km
Speed, v_I	7.95 km/s

Recall that all values are converted to DU, MU, TU, and radians before being used by the algorithms. Now that we have initial and target values, the algorithms can be run and some results obtained.

5.2 Payload Mass to Orbit

The first case considered was one in which the inclination of the rendezvous orbit was equal to the latitude of the launch site, 28.5 degrees for this study. This case was the original case for which LAUNCH was used to determine the initial conditions for the coplanar rendezvous. The payload mass to orbit versus the value of θ_{orb} is shown in

Figure 5-2. The coplanar value has θ_{orb} = 3.306526258 radians with the non-coplanar minimum and maximum values at θ_{orb} = 3.111049382 rad. and θ_{orb} = 3.502003134 rad.

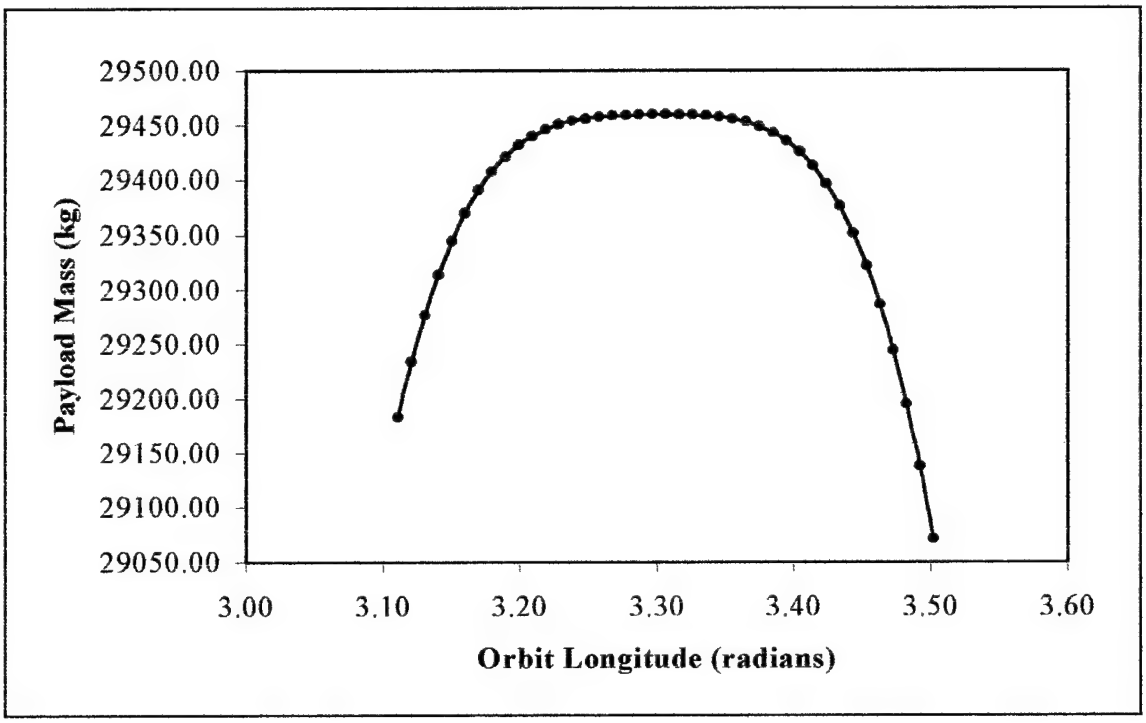

Figure 5-2. Case 1: Payload Mass vs. Orbit Longitude

There are a few items of interest to point out here. First, the largest cost in payload mass is less than 400 kg. This means that the vehicle can deliver a payload to an orbit 11.25-degrees out of the plane for a cost of less than 400 kg. Second, notice how relatively flat the curve is between 3.2 and 3.4 radians. This shows that roughly the same payload mass that can be delivered to the coplanar orbit can also be delivered to orbits +/- approximately six degrees out of the plane. This is significant if the goal is to launch into a particular plane (not necessarily achieve quick rendezvous) because the launch window is now expanded from 1-2 minutes to about 45 minutes allowing more margin for computer glitches, weather problems etc.

The second case considered had the inclination for the rendezvous orbit equal to 35-degrees. The coplanar value for $\theta_{orb} = 3.980123400$ radians and the respective minimum and maximum values were $\theta_{orb} = 3.793591337$ radians and $\theta_{orb} = 4.186290419$ radians. The results for this case are shown below in Figure 5-3.

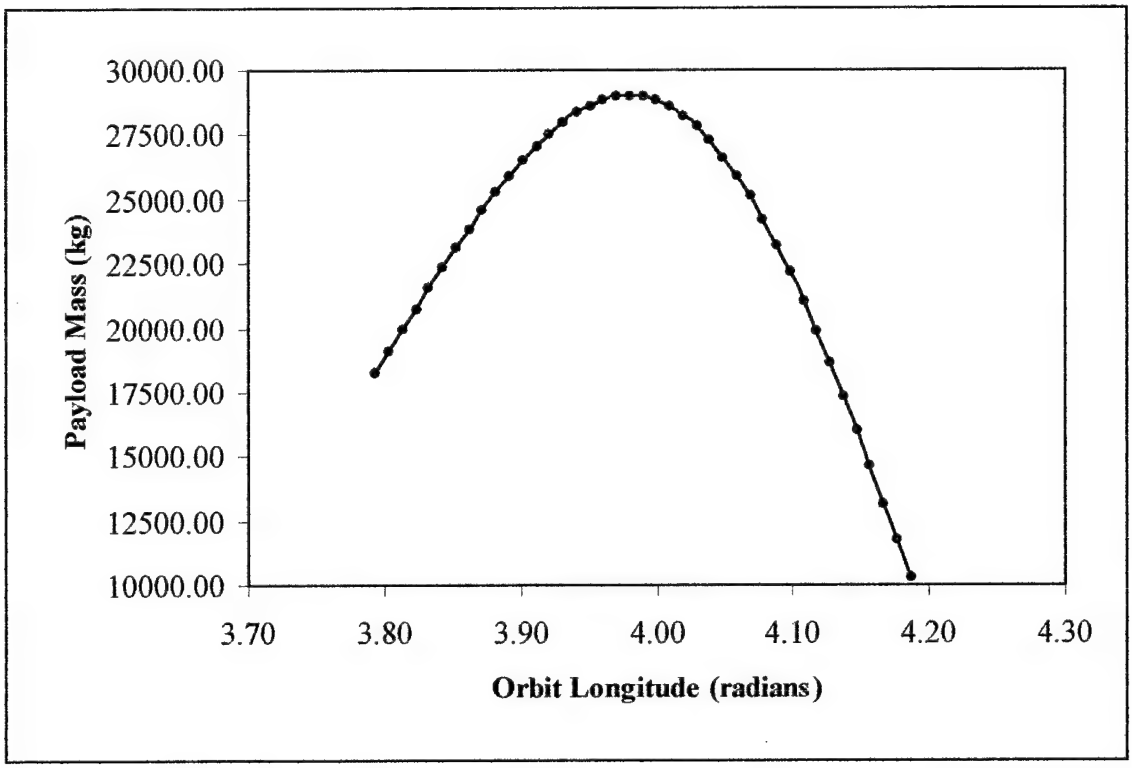

Figure 5-3. Case 2: Payload Mass vs. Orbit Longitude

For this case, the first thing to notice is that while the payload mass to orbit for the coplanar orbit has decreased only slightly, we now pay a much greater payload price for non-coplanar trajectories. The worst case cost is now nearly 19,000 kg to go from the coplanar situation to 11.25-degrees out of the plane. The bright side is that for these circumstances, more than 10,000 kg can be delivered into low earth orbit, 11.25-degrees out of plane, which is still an appreciable amount.

Case number three increased the inclination another ten degrees to 45-degrees. The coplanar value of $\theta_{orb} = 4.293552296$ radians, with respective minimum and maximum values of $\theta_{orb} = 4.107020232$ radians, and $\theta_{orb} = 4.499719314$ radians. The results are below in Figure 5-4.

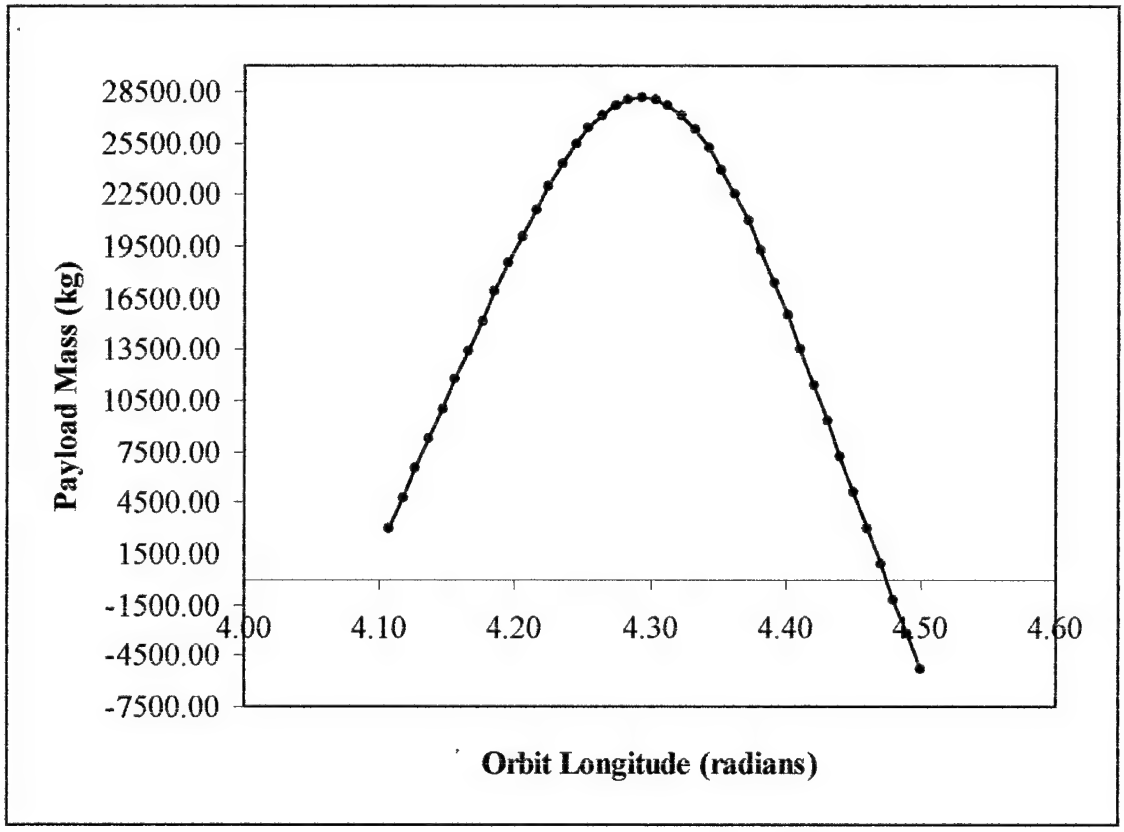

Figure 5-4. Case 3: Payload Mass vs. Orbit Longitude

The results from this plot show not only a decrease in the coplanar mass to orbit (as expected), but even an empty vehicle cannot achieve the same out of plane range that could be done at lower inclinations. The vehicle is getting less help from the earth's rotation as the inclination increases, therefore the final time is increasing as is the amount of fuel required to achieve orbit. The result is a lower payload mass delivered to orbit,

and attempting to reach the non-coplanar trajectories enhances this effect even more. The plot shows that we can only get a payload about 10.2-degrees out of plane instead of the desired 11.25-degrees, for values of θ_{orb} greater than the coplanar value. In addition, the cost per degree of going non-coplanar has increased from the previous cases.

The fourth case was picked to look at a possible rendezvous with a satellite in a 57-degree inclination orbit. The coplanar value for θ_{orb} = 4.516974957 radians, with minimum and maximum values of θ_{orb} = 4.320625417 radians, and θ_{orb} = 4.713324499 radians. The results for this case are shown in Figure 5-5.

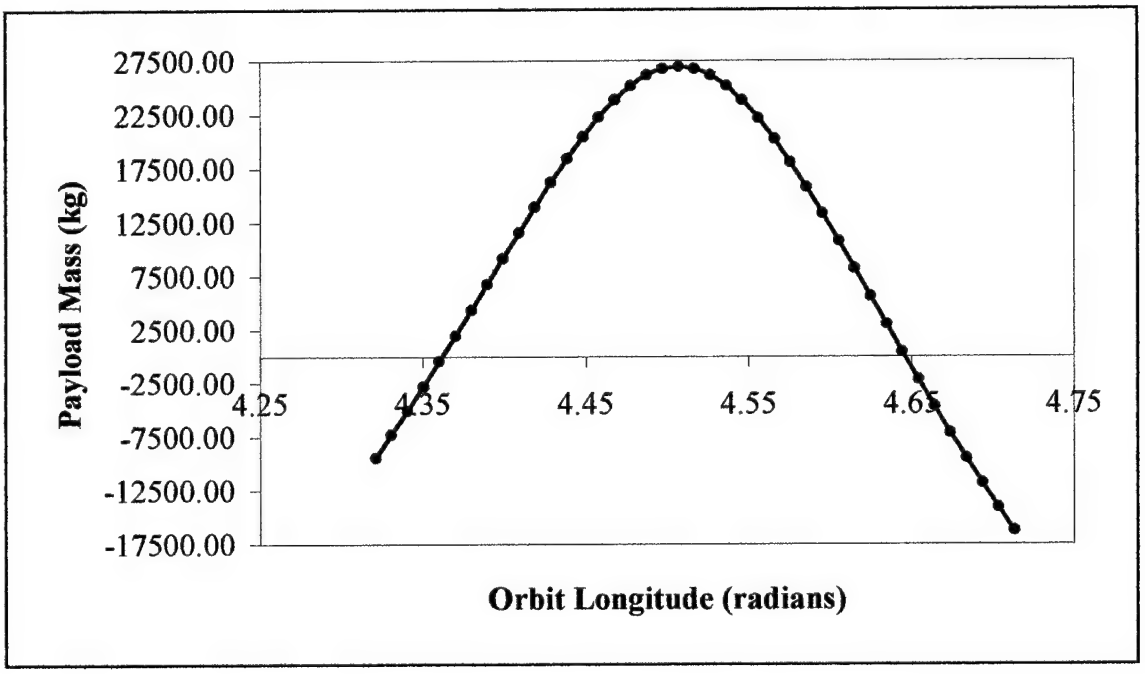

Figure 5-5. Case 4: Payload Mass vs. Orbit Longitude

Again, the same trends occurred as in the previous cases. Slightly less payload mass to orbit for the coplanar case and a higher cost for going non-coplanar. For this

inclination, however, we can get a payload almost 7-degrees out of the plane, which still gives considerable flexibility compared to the way we do things now.

As mentioned earlier, the fifth case was rather unique. Since non-traditional launch methods were being considered, I thought attempting to rendezvous with an orbit whose inclination was less than the latitude of the launch site might provide some interesting results. Case 5 considers rendezvous with a 25-degree inclination orbit from a launch latitude of 28.5-degrees. A modified version of EXTRAPI was used to get the initial solution, which assumed the latitude of the orbit's ground trace reached 25 degrees at the same longitude of the launch site. Once this solution was found, θ_{orb} was varied as in the other cases. The results for this case are below in Figure 5-6.

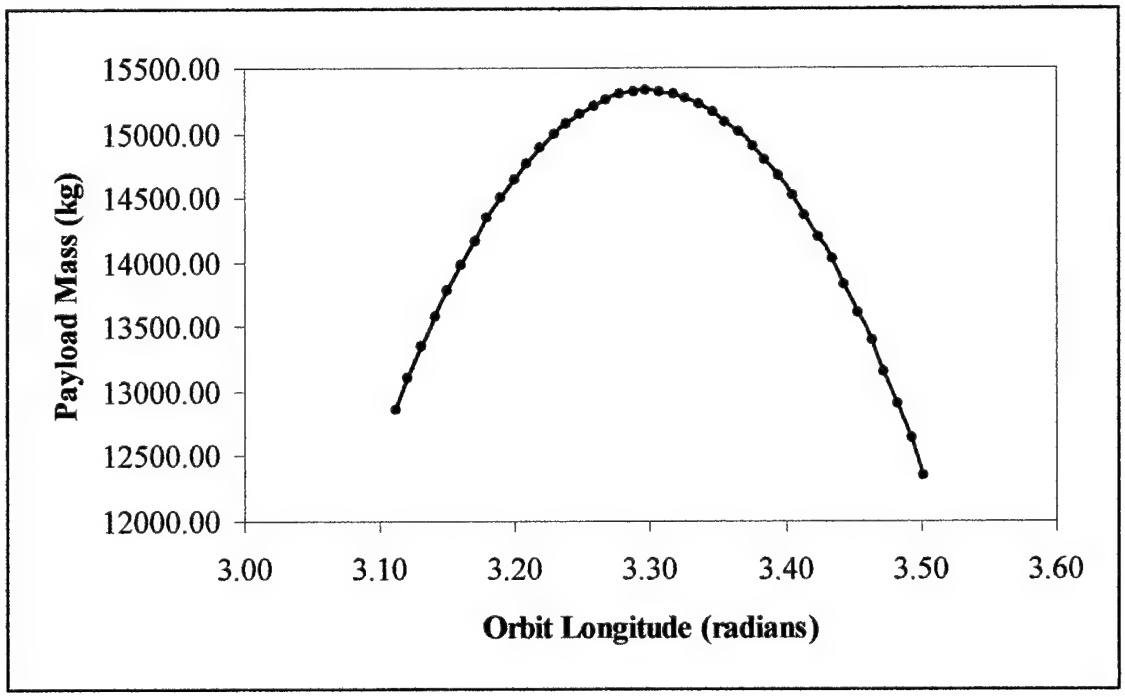

Figure 5-6. Case 5: Payload Mass vs. Orbit Longitude

As can be seen, the results are quite interesting. From 12,000 to 15,000 kg can be delivered over the 22.5-degree range, centered on the launch longitude, 3.5-degrees below the launch latitude. Unfortunately, this good fortune does not continue to the equator. Payload mass fell below zero for inclinations less than 23-degrees. However, this adds another degree of flexibility for attempting to rendezvous with low earth orbiting objects.

5.3 Control Variables

Now that we know what the payload mass is doing for these trajectories, we will take a look at how the control variables, roll and angle of attack, are changing throughout these trajectories. Trajectories for case one and case four will be presented.

For case one, roll and angle of attack were output as a function of time for the coplanar trajectory and for the maximum and minimum non-coplanar trajectories. Figure 5-7 shows roll as a function of time for these three trajectories.

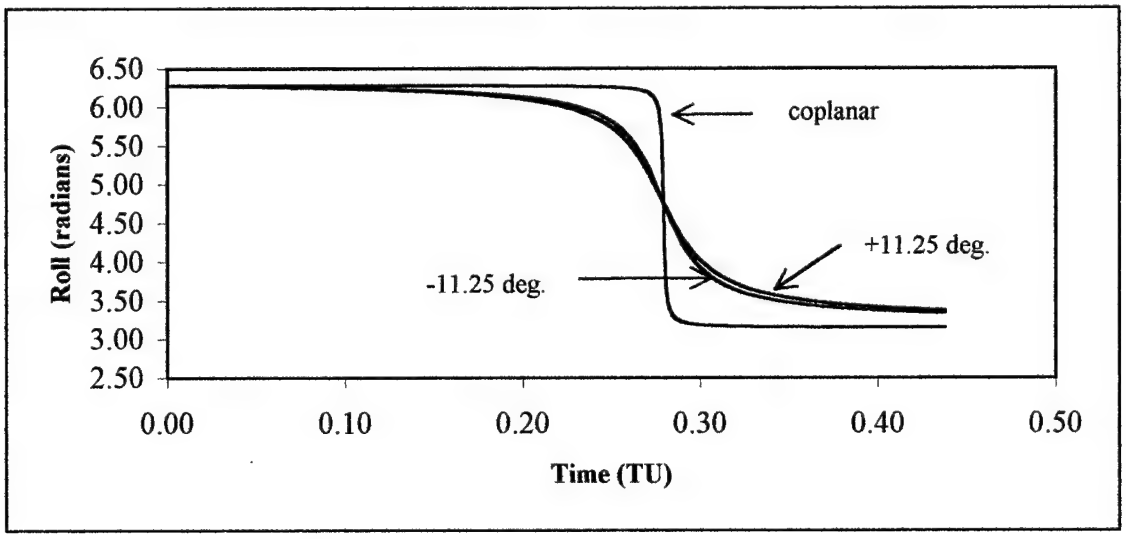

Figure 5-7. Roll vs. Time for Case 1

Notice that for the coplanar case, the vehicle maintained a minute roll to the left, performed a very quick roll of nearly 180 degrees, and then maintained that orientation for the remainder of the trajectory. The two non-coplanar cases performed almost identically and performed a more gradual maneuver throughout the trajectory.

The angle of attack as a function of time for these three trajectories is shown below in Figure 5-8.

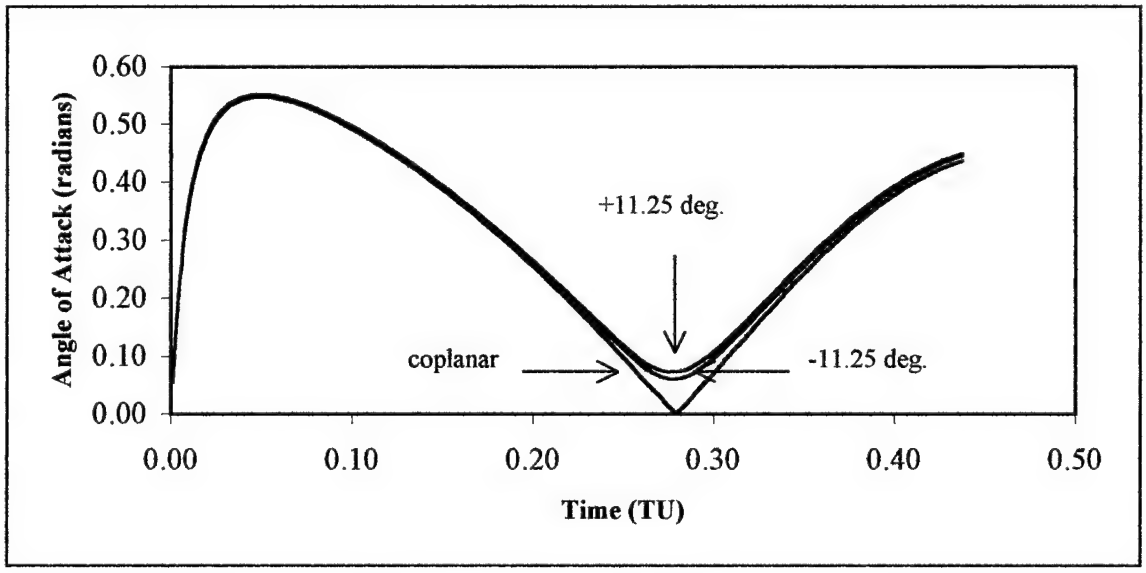

Figure 5-8. Angle of Attack vs. Time for Case 1

The cusp for the coplanar case occurs in conjunction with the sharp roll maneuver as a result of the algorithm. All three of the main programs have a statement in them that only allow positive angles of attack (this will be a constraint for an aerodynamic model). If the angle of attack is calculated negative, a factor of pi is added to the roll and the angle of attack recalculated. This allows the vehicle to follow the optimal trajectory while always presenting the bottom of the vehicle in the direction of the velocity vector.

The two non-coplanar cases, however, do not encounter this and thus have smoother curves for both angle of attack and roll. Another item of interest is that all three trajectories maintain an angle of attack less than 0.552 radians (approx. 31.5 degrees) throughout the trajectories. This is reasonable and presents another 'sanity check' that the vehicle is not maneuvering unrealistically to achieve orbit. In addition, the larger angles of attack occur early in the trajectory, which lends itself nicely to generating lift.

The second case considered was case four, inclination of 57-degrees. Again, the coplanar trajectory was considered, but the minimum and maximum non-coplanar trajectories differ because not all trajectories were achievable. Thus the minimum and maximum were set based on delivering at least 3000 kg payload to orbit. The points satisfying this criteria were $\theta_{orb} = 4.63$ radians and $\theta_{orb} = 4.37$ radians, which convert to plus 6.75 degrees for the maximum and minus 7.8 degrees for the minimum. The results for roll are given in Figure 5-9.

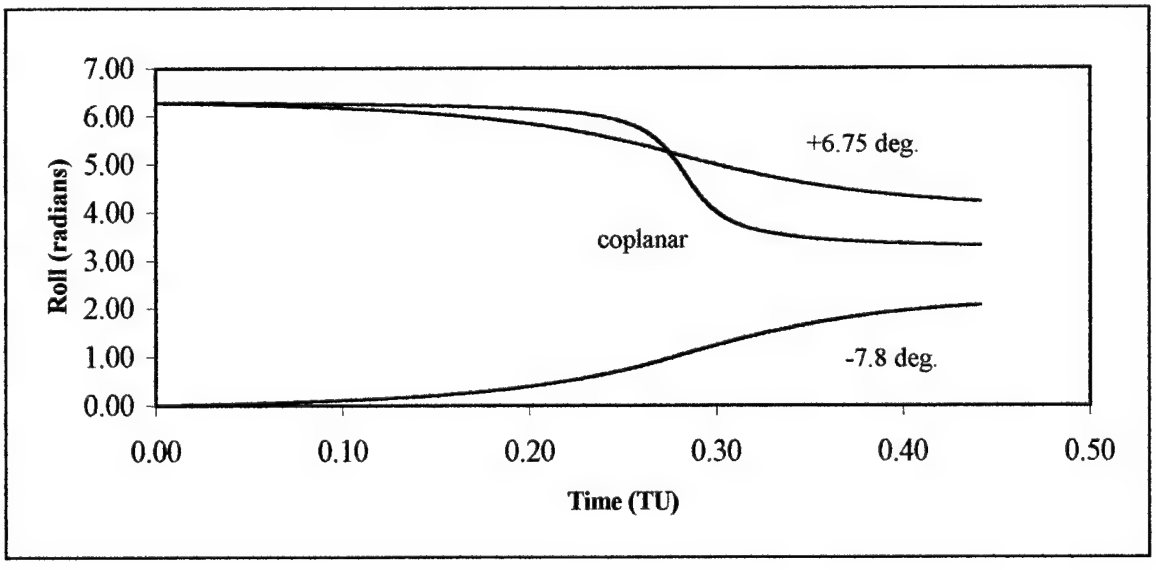

Figure 5-9. Roll vs. Time for Case 4

The roll for the coplanar trajectory is more gradual than for the previous case, but results in roughly the same orientation at the final time. The non-coplanar cases are again very similar however, they rolled in opposite directions. The overall maneuver was smaller than for case one resulting in a different orientation at the final time.

The angle of attack for these three trajectories is shown below in Figure 5-10.

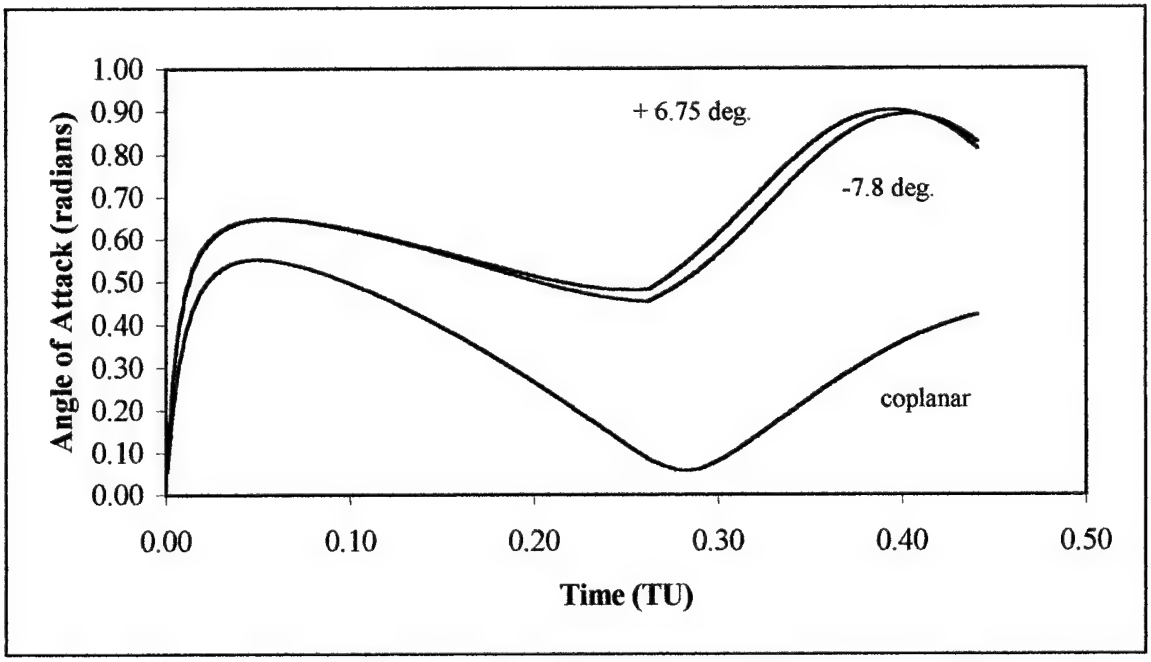

Figure 5-10. Angle of Attack vs. Time for Case 4

The angle of attack for the coplanar trajectory was roughly the same as for case one, however, it didn't try to go negative as before. This could also explain the more gradual roll for this trajectory. The non-coplanar trajectories were again similar to each other however much different from case one. The early angle of attack increased nearly 0.1 radians more than before, declined much less, and increased again to over 0.9 radians (more than 50 degrees) near the final time. This was due to the different geometry that

resulted from the increase in inclination. Also, it is not necessarily infeasible since the vehicle would not be confronting any appreciable aerodynamic forces at that point in the trajectory.

As has been shown in the previous two sections, launching on non-coplanar trajectories is not an infeasible idea. Very reasonable payload masses were attained for the cases presented. In addition, the roll and angle of attack of the vehicle as it followed these trajectories were completely realistic. The next chapter presents the results for the second scenario considered. This scenario had the vehicle ascend through the atmosphere on a gravity turn trajectory (roll and angle of attack equal zero) and begin the optimal control portion once the dynamic pressure on the vehicle is negligible.

VI. GRAVITY TURN RESULTS

6.1 Introduction

This chapter presents the results obtained from the vehicle following a gravity turn trajectory until it was out of the atmosphere and beginning the optimal control portion of the trajectory at that point. A gravity turn trajectory is one in which roll and angle of attack are maintained at zero. Since these two angles are zero, no lift can be generated, however, drag is now present. This launch method is used by current launch vehicles to achieve orbit therefore any current launch vehicle could potentially follow the trajectories described in this chapter.

The three main programs had to be modified to accommodate the gravity turn portion of the trajectory. The duration of the gravity turn portion had to be determined as well as the inclusion of the atmospheric and aerodynamic models. The time at which the vehicle began the optimal control portion of the trajectory was established by determining the time when the dynamic pressure on the vehicle was approximately 0.1 pounds per square inch. This occurred at approximately 0.24 TU into the trajectory (shortly before the throttle back time). This time was then used for all of the trajectories considered.

The atmospheric modeling was accomplished through the use of the subroutine ATM. This subroutine was developed and detailed by Platt[5, 11-13]. It models the atmosphere from 0 to 700-km dividing it into 21 discrete altitude bands. Given the air pressure at sea level and an altitude, this subroutine returned the atmospheric density for the given altitude. It provided a standard atmospheric model but did not take into account

variations due to increased solar activity or effects of winds on pressure in a particular region.

The coefficients of lift and drag were calculated using the subroutine AERO. AERO was developed by Dr. Wiesel and returned the coefficients of lift and drag given an angle of attack and lift and drag data specific to the vehicle used in the model. This data for the DC-Y was presented earlier in Figure 1-3. Using the results from AERO and ATM, lift and drag forces could be calculated and include in the model.

The final necessary modification was that the initial time of the problem and the initial time of the optimal control portion were now different. Since the programs were making corrections to the free variables at the initial time, it was necessary to distinguish which variables were to be corrected at which time. This was accomplished by correcting all of the free variables at t_0. Only the seven state values were passed to HAMING for integration during the gravity turn portion; the seven co-state values were set to zero. This could be accomplished because no optimal control was being performed during the gravity turn portion. At the end of the gravity turn portion, the current (integrated through the gravity turn portion) values of the state variables were coupled with the initial (or corrected) values of the co-state variables. These 14 values were passed to HAMING to begin the integration of the optimal control portion and integrated as in the previous chapter to the determined final time. The result of this corrected the flight path angle, the heading angle, and the value for the final time at t_0 and corrected the free co-state variables at the end of the gravity turn portion of the trajectory.

The same five inclination cases that were considered in chapter 5 were repeated here. In addition the values presented in Tables 5-1 and 5-2 also apply to this scenario.

6.2 Payload Mass to Orbit

The first case considered was the rendezvous to a 28.5-degree orbit from a launch latitude of 28.5 degrees. The coplanar value had $\theta_{orb} = 3.306526258$ radians with the non-coplanar minimum value of $\theta_{orb} = 3.111049382$ radians and maximum value of $\theta_{orb} = 3.502003134$ radians. Figure 6-1 compares the payload mass to orbit for both the gravity turn and non-aerodynamic scenarios.

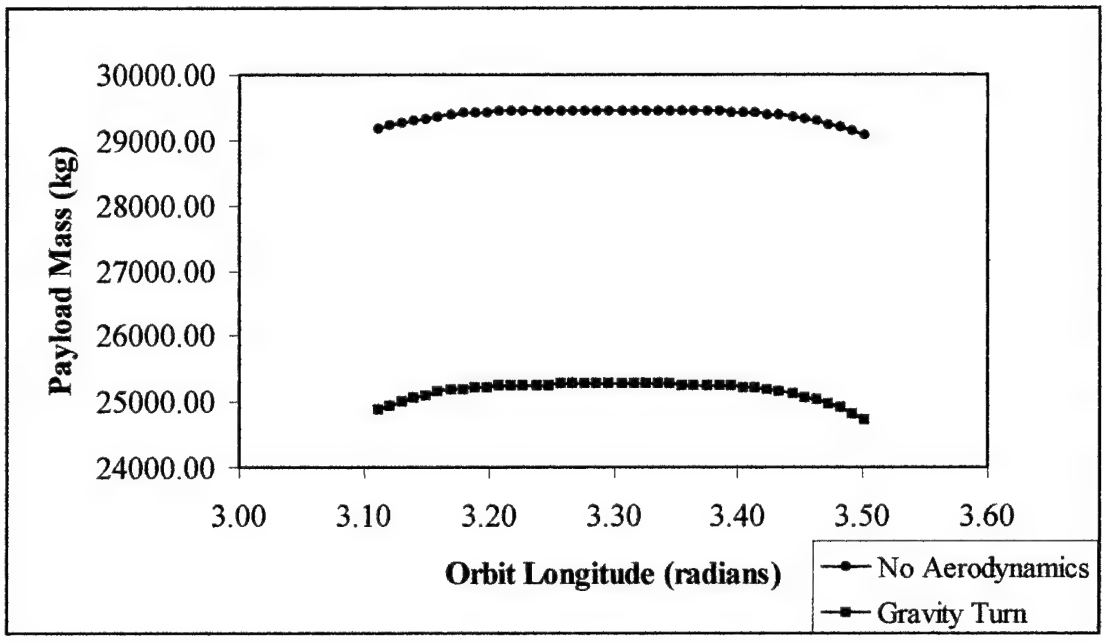

Figure 6-1. Case 1: Payload Mass vs. Orbit Longitude

Just as in the non-aerodynamic scenario, the maximum cost in payload mass to deliver a payload 11.25 degrees out of the plane was relatively small, about 500 kg in this case. Again, the curve was relatively flat between and the total payload deliverable was relatively large. Adding drag to the model resulted in an additional cost in payload mass

of about 4000-kg over the non-aerodynamic scenario, which was relatively consistent across the entire 22.5-degree range of orbit longitude.

The second case considered was a rendezvous orbit at 35 degrees inclination. The coplanar value for $\theta_{orb} = 3.980123400$ radians and the respective minimum and maximum values were $\theta_{orb} = 3.793591337$ radians and $\theta_{orb} = 4.186290419$ radians. The results for this case are shown below in Figure 6-2.

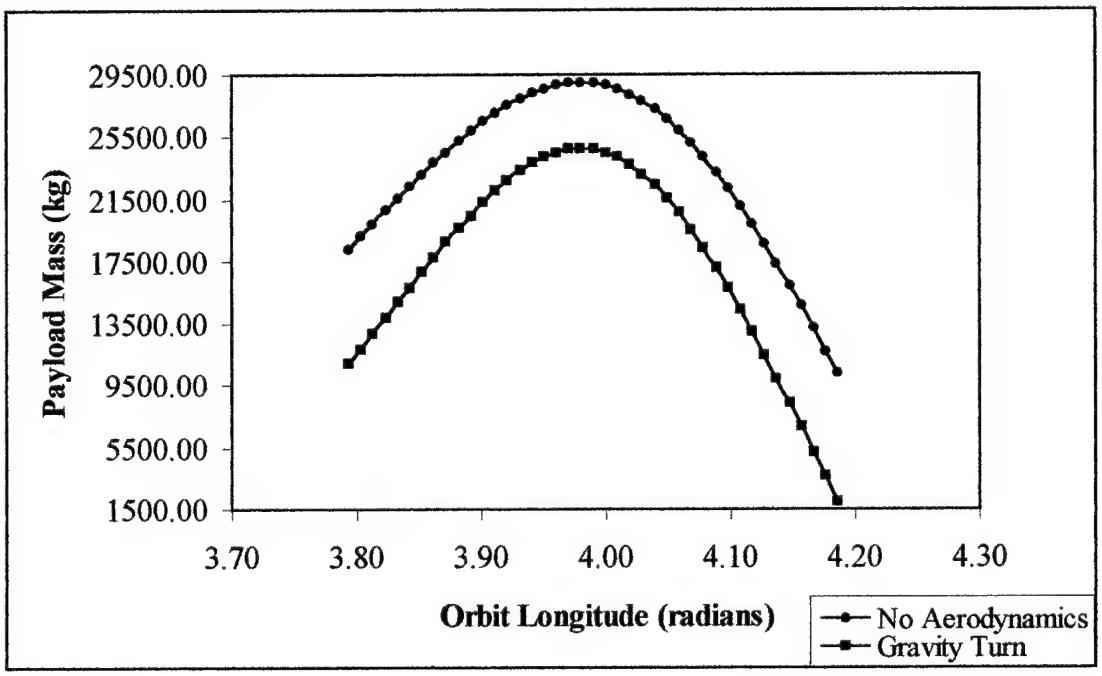

Figure 6-2. Case 2: Payload Mass vs. Orbit Longitude

Figure 6-2 shows that the cost in payload mass had become much larger for the gravity turn scenario. We were still able to get a payload to orbit across the entire 22.5-degree range, however, it was much smaller than the non-aerodynamic scenario. Notice also that while the difference between the coplanar orbits remained about 4000-kg, the

difference was approximately 8000-kg for the far non-coplanar orbits. It has gotten more expensive to get to the non-coplanar orbits.

The third case looked at a rendezvous orbit with an inclination of 45 degrees. The coplanar value was $\theta_{orb} = 4.293552296$ radians, with respective minimum and maximum values of $\theta_{orb} = 4.107020232$ radians, and $\theta_{orb} = 4.499719314$ radians. The compared results are below in Figure 6-3.

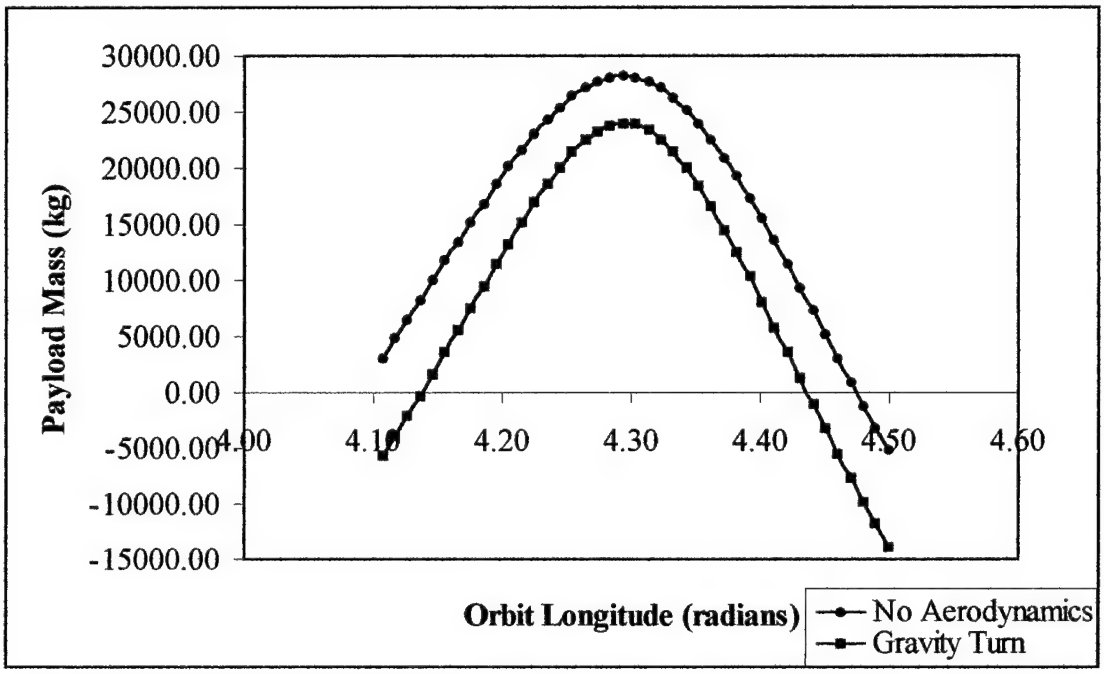

Figure 6-3. Case 3: Payload Mass vs. Orbit Longitude

As before, we lost the ability to span the entire range of orbit longitudes. For the gravity turn case, we could only go about 7.5 degrees as opposed to the 10 degrees for the non-aerodynamic scenario. The increasing mass difference between the two scenarios that was noted in the previous case continued with this case.

The fourth case was picked to mimic a possible space station rendezvous at an inclination of 57 degrees. The coplanar value for θ_{orb} = 4.516974957 radians, with minimum and maximum values of θ_{orb} = 4.320625417 radians, and θ_{orb} = 4.713324499 radians. The results for this case are shown in Figure 6-4.

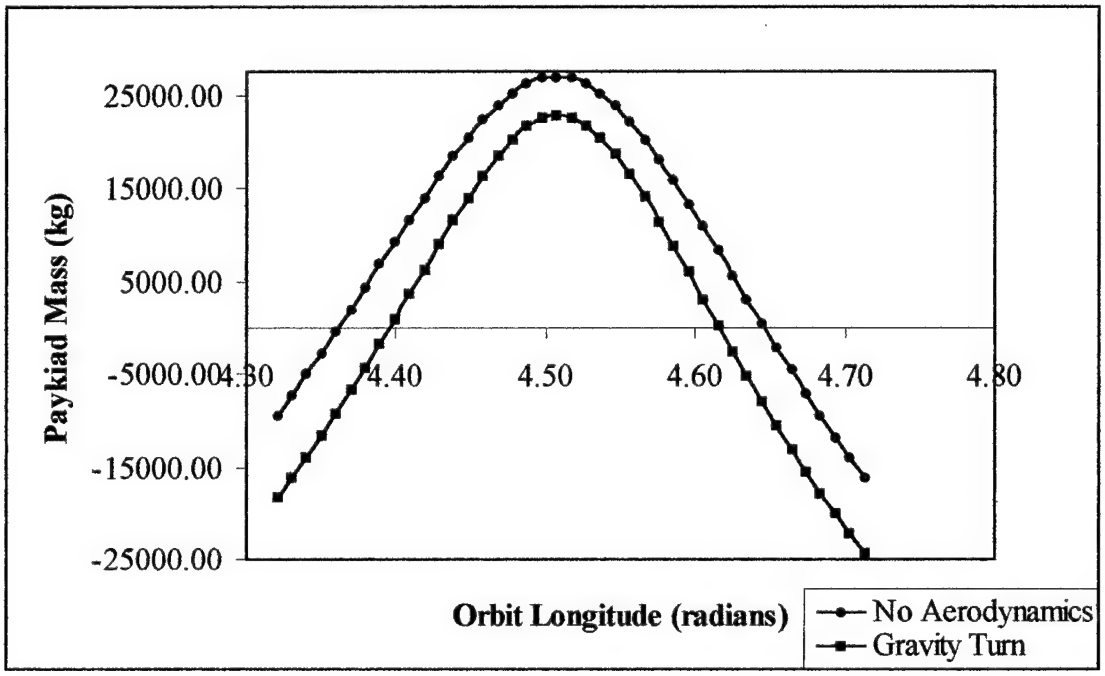

Figure 6-4. Case 4: Payload Mass vs. Orbit Longitude

The same trends that appeared in the previous scenario also appeared for this case. Payload mass decreased with inclination and the far non-coplanar orbits that were reachable for lower inclinations were not possible here. For the non-aerodynamic scenario, we were able to launch a payload almost 7 degrees out of the plane and for the gravity turn scenario, that value has dropped to about 5.75 degrees. This result was still attractive in that for a rescue mission, very little payload must be delivered. In addition, we still had access to over half of the 22.5-degree non-coplanar range.

The final case was an attempt to reach a 25-degree inclination orbit as described in the previous chapter. The results for the gravity turn scenario are compared to the non-aerodynamic results in Figure 6-5.

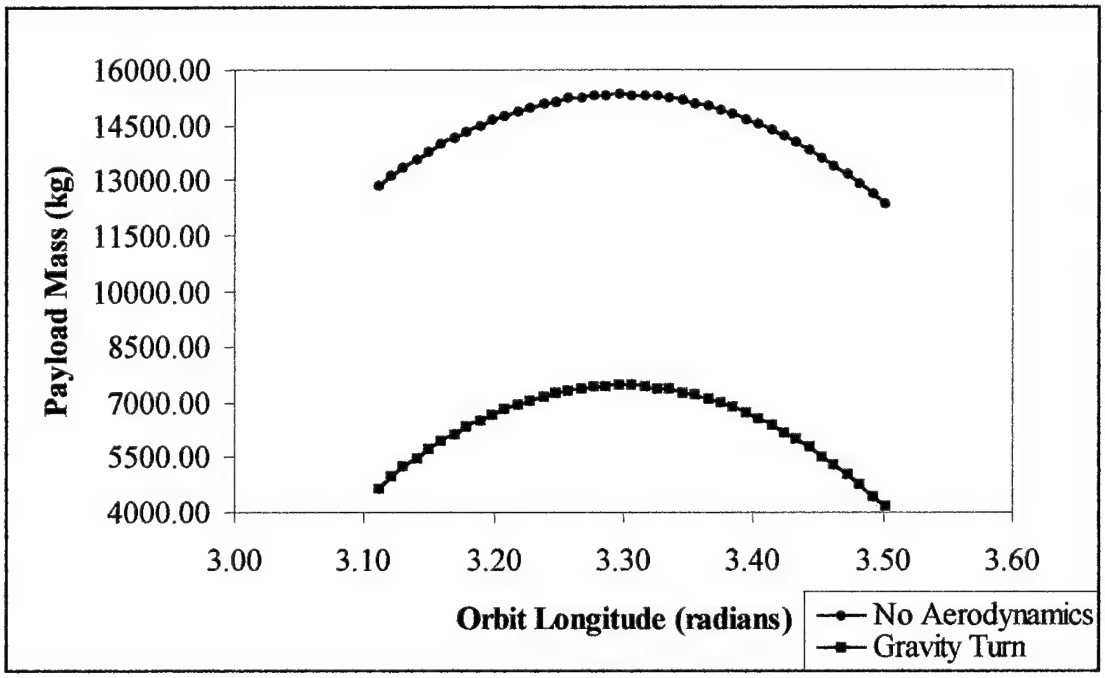

Figure 6-5. Case 5: Payload Mass vs. Orbit Longitude

The results for this case were very reasonable. Between 4100 and 7500-kg could be delivered over the 22.5 degree range for the gravity turn scenario. This was almost 8000-kg less than for the non-aerodynamic scenario, however this was still an appreciable amount. As with the no-aerodynamic scenario, payload masses decreased quickly as inclination decreased, and inclinations below 23 degrees could not be reached.

6.3 Control Variables

For the gravity turn scenario, the control variables were examined as a function of time for the 28.5-degree inclination case (case 1) and the 57-degree inclination case (case 4). Beginning with case 1, Figure 6-6 shows roll as a function of time for the coplanar trajectory as well as the minimum and maximum non-coplanar trajectories which occurred at –11.25 degrees and + 11.25 degrees respectively.

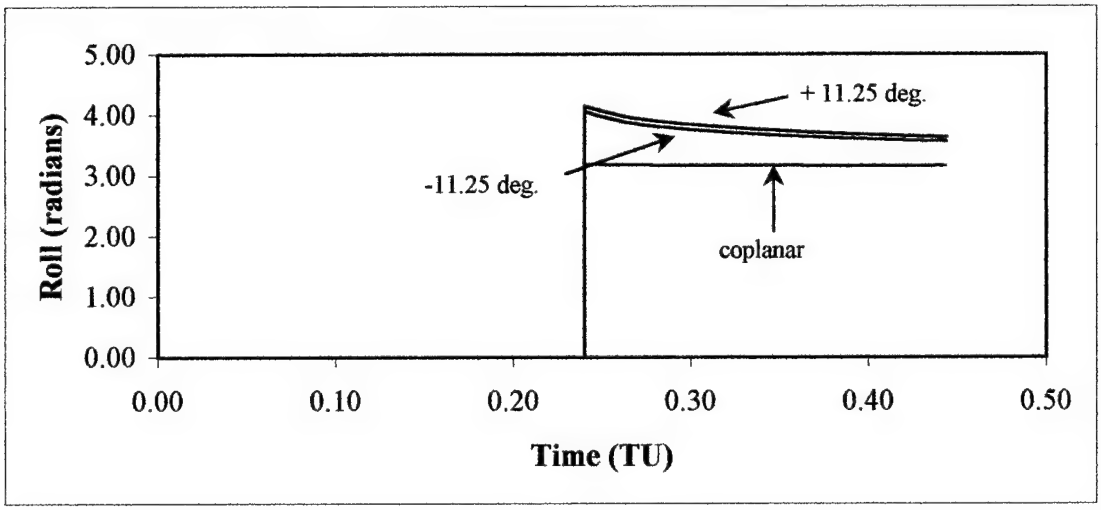

Figure 6-6. Roll vs. Time for Case 1

The vehicle performed a roll maneuver during all three trajectories as soon as the gravity turn portion of the trajectory was completed. For the coplanar trajectory, the vehicle almost inverted itself to a roll value of approximately 3.18 radians, which decreased to 3.15 radians at the final time. While following the two non-coplanar trajectories, the vehicle performed roughly the same maneuver at the end of the gravity turn portion with the value of the roll decreasing roughly 0.5 radians to the final time. The difference in values between the two was approximately 0.1 radians, which was maintained throughout the optimal control portion of the trajectory.

The angle of attack as a function of time for all three trajectories is shown in Figure 6-7.

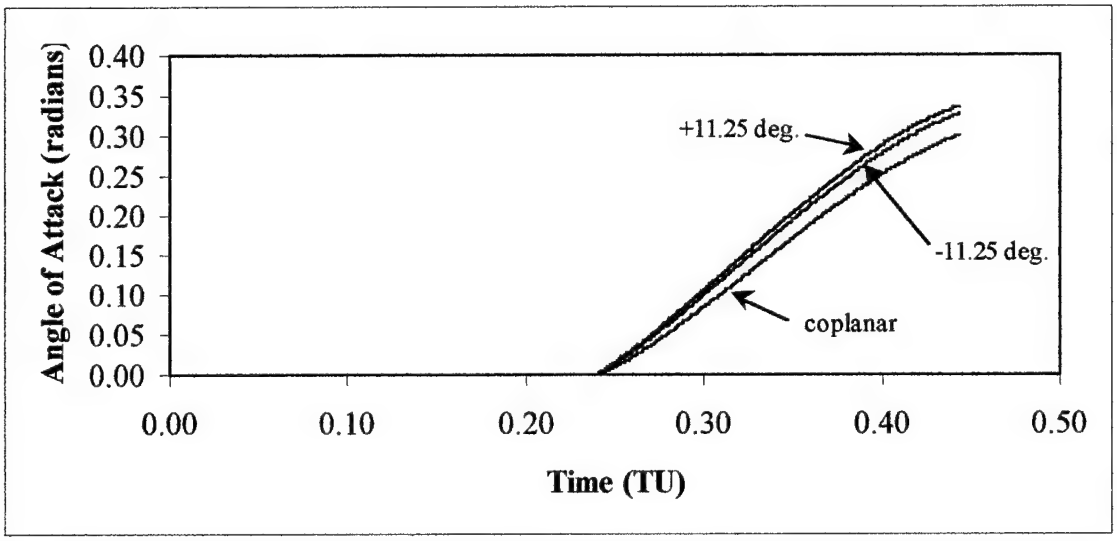

Figure 6-7. Angle of Attack vs. Time for Case 1

Compared to the values for the non-aerodynamic scenario (Figure 5-8), these results exhibited some similar characteristics. All three trajectories showed nearly linear increases in the angle of attack throughout the latter portion of each trajectory (> .29 TU). The values of angle of attack were larger for the non-coplanar trajectory and the largest values were required for the +11.25-degree trajectory. Some differences were that for this scenario, there was more of a difference between the coplanar and non-coplanar curves. In addition, the final values for angle of attack were approximately 0.1 radians less than the values for the non-aerodynamic scenario.

Next, we move to the 57-degree inclination case, case 4. Just as in the non-aerodynamic scenario, the minimum and maximum non-coplanar trajectories had to be determined based on delivery of approximately 3000-kg of payload to orbit. For the

gravity turn scenario, this set the minimum value for orbit longitude at $\theta_{orb} = 4.408$ radians and the maximum value for orbit longitude at $\theta_{orb} = 4.605$ radians. This equated to roughly 5.8 degrees for the minimum and 5.4 degrees for the maximum. The results for roll as a function of time are given in Figure 6-8.

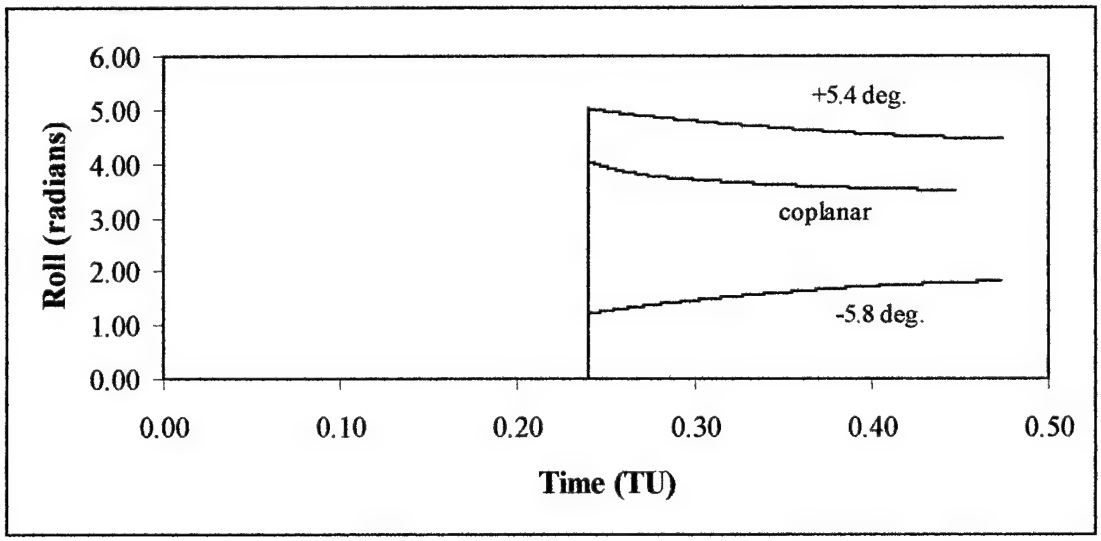

Figure 6-8. Roll vs. Time for Case 4

The results from this scenario were very similar to the non-aerodynamic scenario (Figure 5-9). The vehicle performed gradual rolls to the left during the coplanar and +5.4-degree trajectories while the vehicle performed a gradual roll to the right during the –5.8-degree trajectory just as it did for the non-aerodynamic scenario. Another interesting result for this scenario was that the overall roll maneuver performed during all three trajectories was very similar to those performed along the non-coplanar trajectories for case 1 above. An initial value was attained after the gravity turn portion, and the vehicle continued in a gradual roll to the final time.

The angle of attack as a function of time for the three trajectories of case 4 is shown below in Figure 6-9.

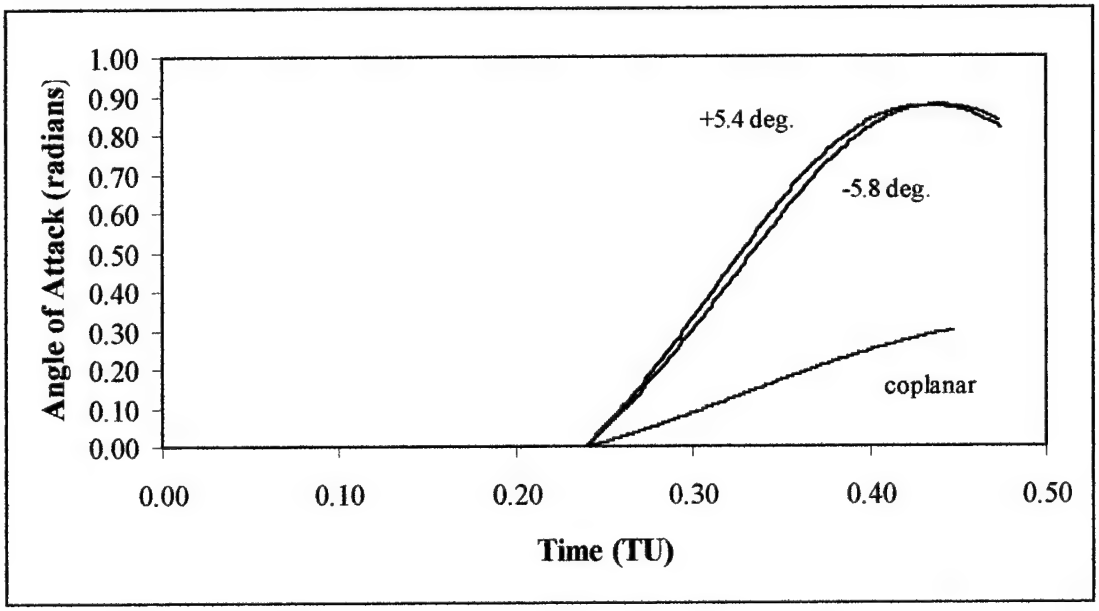

Figure 6-9. Angle of Attack vs. Time for Case 4

Once again similar results were obtained compared to the non-aerodynamic scenario (Figure 5-10). Very different behavior was observed between the coplanar and non-coplanar trajectories. A nearly linear increase to a relatively small value of angle of attack was observed for the coplanar trajectory. The non-coplanar trajectories showed a rather steep increase in angle of attack to almost 1 radian peaking shortly before the final time.

The results from this section showed that while the actual values of roll and angle of attack were different for the gravity turn scenario compared to the non-aerodynamic scenario, the values for each trajectory relative to each other for the different cases remained almost identical. In other words, the shapes of the curves were roughly the

same for the two cases independent of the scenario for times greater than 0.29 TU. For a given case, the vehicle performed roughly same maneuvers along the non-coplanar trajectories relative to the coplanar trajectory and ended up in roughly the same orientation.

This chapter demonstrated again that reasonable payload masses could be launched and reasonable values for roll and angle of attack utilized to follow non-coplanar trajectories to quick rendezvous. In addition, the gravity turn method through the atmosphere scenario is used by current launch vehicles. Adding the optimal control portion outside the atmosphere, therefore, makes this scenario feasible for current launch vehicles as well. Some final conclusions and recommendations for further study will be presented in the next chapter.

VII. CONCLUSIONS AND RECOMMENDATIONS

7.1 Conclusions

The goal of this research was to determine the feasibility of optimal, non-coplanar launch to rendezvous and to examine the cost, in payload mass, of following such trajectories. The results from the last two chapters demonstrated that not only was following these trajectories feasible, but that the cost, in terms of payload mass, was not outrageous. In fact, the capability demonstrated by this technique to deliver a 3000-kg payload to low earth orbit, 5.5 degrees out of the plane, at an inclination of 57°, paves the way for much more flexibility in the way certain launch operations could be conducted. For example, if the goal were simply to launch to a particular orbital plane, launch windows would be much more flexible. In addition, for those orbits that were reachable, the capability of 'popping-up' next to the target at burnout would improve the success rate for time critical missions.

All of the cases considered for this study could be valid scenarios for launches from the Eastern Range. Cases one, two, and five demonstrated that the vehicle (and an appreciable payload) could reach orbit across the entire 22.5° range. In other words, the vehicle could be launched for a direct rendezvous with the 'target' because the 'target' orbit would be accessible throughout the entire 90-minutes required to orbit the earth once. Therefore, the launch time would be dictated by when the 'target' vehicle was in proper phase with the launch site within the 22.5° range. This would facilitate a direct launch to rendezvous within (at worst) 24-hours from the need arising, assuming the vehicle was prepared for launch. While cases three and four could not reach across the

entire 22.5° range from this single launch facility, adding a second launch facility with overlapping coverage would allow quick rendezvous across the 22.5° range for the higher inclination orbits as well..

In addition to the payload mass results, analysis of the control variables provided some valuable insight. Although only results for cases one and four were presented, they indicated that the values for roll and angle of attack throughout the trajectory were within acceptable levels. In other words, the mathematics was not saying that the optimal method to achieve the specified orbit was to orient the vehicle perpendicular to the velocity vector. The values were consistent with requisite orientations for a vehicle attempting to reach orbit. This added further support to the conclusion that launching on these non-coplanar trajectories is feasible.

7.2 Recommendations

The obvious next step is to remove the gravity turn restriction in the atmosphere. Although the results from this research are exciting, the true validity of this technique will only be realized by extending the optimal control through the atmospheric portion of the trajectory. Recall that the vehicle selected for this study was chosen for the relatively high lift-to-drag ratio compared to other current SSTO designs. The model as presented here does not exploit this advantage. The results are not expected to differ significantly from those presented here because of this and the fact that the vehicle is only in the atmosphere less than 25% of the total trajectory. Unfortunately, problems resulting from trying to incorporate the optimal control with the atmospheric and aerodynamic models were unresolved in time for inclusion in this thesis.

Another interesting result warranting further examination comes from the plots of payload mass presented in the previous chapters. The first thing that catches the eye is that the curves are asymmetric. The asymmetry itself can be attributed to the rotation of the earth. This was determined by running EXTRAP with the value of the earth's rotation, ω, set to zero. The result was a perfectly symmetric curve with the maximum mass value coming from the coplanar trajectory. The plots from chapters five and six have a maximum mass value from the first non-coplanar trajectory to the west of the coplanar trajectory. This may be a result of the inability to define a truly coplanar launch trajectory, but could be influenced by other factors. In addition, the plots indicate that it costs more payload mass to go eastward than westward. This is counter-intuitive has no explanation at this time. Further study of these trajectories and further analysis of what the vehicle is actually doing along the trajectories may explain this phenomenon.

The missions and activities of humans in space are continually evolving. As a result, cheaper and more efficient methods for launching into space must also evolve. The results of this thesis effort demonstrate a step in this evolution. The ability to launch directly to rendezvous with an orbiting object within 24-hours, while keeping the cost in payload mass reasonable is a very desirable goal. It saves both waiting times on the ground and time in orbit by not having to play catch-up. This in turn reduces the overall monetary cost of such missions. The technique outlined here opens up some interesting and exciting possibilities for the future of space travel.

APPENDIX A: Co-State Equations of Motion

Each of these equations of motion is obtained by taking the negative of the partial derivative of the Hamiltonian with respect to the respective state. In equation form this means $\dot{\lambda}_i = -\frac{\partial H}{\partial x_i}$. The Hamiltonian, equation 3-22, is reproduced here for convenience.

$$H(t)=1+\left\{\begin{array}{l}\lambda_r(v\sin\gamma)+\lambda_\theta\left(\frac{v\cos\gamma\sin\psi}{r\cos\phi}\right)+\lambda_\phi\left(\frac{v\cos\gamma\cos\psi}{r}\right)\\ +\lambda_v\left(\frac{T\cos\alpha}{m}-\frac{c_D S\rho v^2}{2m}-g\sin\gamma\right)\\ +\lambda_\gamma\left(\frac{T\sin\alpha\cos\sigma}{mv}+\frac{c_L S\rho v\cos\sigma}{2m}-\frac{g\cos\gamma}{v}+\frac{v\cos\gamma}{r}+2\omega\cos\phi\sin\psi\right)\\ +\lambda_\psi\left(\frac{T\sin\alpha\sin\sigma}{mv\cos\gamma}+\frac{c_L S\rho v\sin\sigma}{2m\cos\gamma}+\frac{v\cos\gamma\sin\psi\tan\phi}{r}+2\omega(\sin\phi-\cos\phi\cos\psi\tan\gamma)\right)\\ +\lambda_m\beta\end{array}\right\} \quad \text{(A-1)}$$

The first equation of motion for $\dot{\lambda}_r$ is given by:

$$\dot{\lambda}_r = -\frac{\partial H}{\partial r} = \left\{\begin{array}{l}\frac{\lambda_\theta v\cos\gamma\sec\phi\sin\psi}{r^2}+\frac{\lambda_\phi v\cos\gamma\cos\psi}{r^2}+\frac{\lambda_v c_D S v^2\rho'}{2m}\\ -\lambda_\gamma\left[\left(\frac{c_L S\rho' v\cos\sigma}{2m}\right)-\left(\frac{v\cos\gamma}{r^2}\right)\right]\\ -\lambda_\psi\left[\left(\frac{c_L S\rho' v\sec\gamma\sin\sigma}{2m}\right)-\left(\frac{v\cos\gamma\sin\psi\tan\phi}{r^2}\right)\right]\end{array}\right\} \quad \text{(A-2)}$$

where ρ' is the derivative of air density (which is a function of altitude and therefore r) with respect to r.

Since θ does not appear explicitly in the Hamiltonian, the equation for $\dot{\lambda}_\theta$ is trivial and is written as:

$$\dot{\lambda}_\theta = -\frac{\partial H}{\partial \theta} = 0. \tag{A-3}$$

The third equation, which gives $\dot{\lambda}_\phi$, can be written as:

$$\dot{\lambda}_\phi = -\frac{\partial H}{\partial \phi} = \begin{Bmatrix} 2\lambda_\gamma \omega \sin\phi \sin\psi \\ -\lambda_\psi \left[\dfrac{v \cos\gamma \sec^2\phi \sin\psi}{r} + 2\omega(\cos\phi + \sin\phi \cos\psi \tan\gamma) \right] \end{Bmatrix} \tag{A-4}$$

The fourth equation determines the equation of motion for $\dot{\lambda}_v$, which is given as:

$$\dot{\lambda}_v = -\frac{\partial H}{\partial v} = -\begin{Bmatrix} \lambda_r \sin\gamma + \lambda_\theta \left(\dfrac{\cos\gamma \sin\psi \sec\phi}{r} \right) + \lambda_\phi \left(\dfrac{\cos\gamma \cos\psi}{r} \right) \\ -\lambda_v \left(\dfrac{c_D S \rho v}{m} \right) \\ +\lambda_\gamma \left[-\left(\dfrac{T \sin\alpha \cos\sigma}{mv^2} \right) + \dfrac{c_L S \rho \cos\sigma}{2m} + \dfrac{g \cos\gamma}{v^2} + \dfrac{\cos\gamma}{r} \right] \\ +\lambda_\psi \left[-\left(\dfrac{T \sin\alpha \sin\sigma \sec\gamma}{mv^2} \right) + \dfrac{c_L S \rho \sin\sigma \sec\gamma}{2m} + \dfrac{\cos\gamma \sin\psi \tan\phi}{r} \right] \end{Bmatrix} \tag{A-5}$$

The next equation yields the equation of motion for $\dot{\lambda}_\gamma$ as:

$$\dot{\lambda}_\gamma = -\frac{\partial H}{\partial \gamma} = \begin{Bmatrix} -\lambda_r v \cos\gamma + \lambda_\theta \left(\dfrac{v \sin\gamma \sin\psi \sec\phi}{r} \right) + \lambda_\phi \left(\dfrac{v \sin\gamma \cos\psi}{r} \right) \\ +\lambda_v g \cos\gamma - \lambda_\gamma \left(\dfrac{g \sin\gamma}{v} - \dfrac{v \sin\gamma}{r} \right) \\ -\lambda_\psi \left(\dfrac{T \sin\alpha \sin\sigma \sec\gamma \tan\gamma}{mv} + \dfrac{c_L S \rho v \sin\sigma \sec\gamma \tan\gamma}{2m} \right) \\ +\lambda_\psi \left(\dfrac{v \sin\gamma \sin\psi \tan\phi}{r} + 2\omega \cos\phi \cos\psi \sec^2\phi \right) \end{Bmatrix} \tag{A-6}$$

The sixth co-state equation of motion is:

$$\dot{\lambda}_{\psi} = -\frac{\partial H}{\partial \psi} = \begin{Bmatrix} -\lambda_{\theta}\left(\frac{v\cos\gamma\cos\psi\sec\phi}{r}\right) + \lambda_{\phi}\left(\frac{v\cos\gamma\sin\psi}{r}\right) \\ -2\lambda_{\gamma}\omega\cos\phi\cos\psi \\ -\lambda_{\psi}\left(2\omega\cos\phi\sin\psi\tan\gamma + \frac{v\cos\gamma\cos\psi\tan\phi}{r}\right) \end{Bmatrix} \qquad \text{(A-7)}$$

As mentioned in Chapter three, the value of λ_m was not important to the problem and was set to zero from the initial time to the final time. Therefore the final co-state equation of motion is:

$$\dot{\lambda}_{m} = -\frac{\partial H}{\partial m} = 0 \qquad \text{(A-8)}$$

Equations A-2 through A-8 represent the seven co-state equations of motion that were utilized by the model to determine the values for the Lagrange multipliers from the initial time to the final time.

Bibliography

1. Bate, Roger R., Donald D. Mueller, and Jerry E. White. Fundamentals of Astrodynamics. New York: Dover Publications, Inc., 1971.

2. Bryson, Arthur E., Jr., and Yu-Chi Ho. Applied Optimal Control: Optimization, Estimation, and Control. Washington D.C.: Hemisphere Publishing Corporation, 1975.

3. Larson, Wiley J., and James R. Wertz (editors). Space Mission Analysis and Design (second edition). Torrance, California: Microcosm, Inc. 1992.

4. Lipschutz, Seymour, and Arthur Poe. Schaum's Outline of Theory and Problems of Programming with Fortran Including Structured Fortran. New York: McGraw-Hill, Inc., 1978.

5. Platt, Michael H. Full Lyapunov Exponent Placement in Reentry Trajectories. MS Thesis, AFIT/GA/ENY/95D-03. School of Engineering, Air Force Institute of Technology (AU), Wright-Patterson AFB, OH, December 1995 (AD-A303109).

6. Vinh, Nguyen X., Adolf Busemann, and Robert D. Culp. Hypersonic and Planetary Entry Flight Mechanics. Ann Arbor: University of Michigan Press, 1975.

7. Wiesel, William E. Spaceflight Dynamics. New York: McGraw-Hill, Inc., 1989.

Vita

Captain Gregory B. Sears was born December 17th, 1968 in Akron, Ohio. He graduated in 1986 from Wooster High School, Wooster, OH, and received his B.S. in Astronomy and Astrophysics from Indiana University in 1990. He entered the Air Force in September, 1992 and was commissioned in February, 1993 after completing Officer Training School.

His first tour of duty was served in Colorado Springs, Colorado. From 1993-1994, he served as Deputy Commander, Missile Warning Center, Cheyenne Mountain AS, CO. From 1994-1996, he served as Instructor, Missile Warning Training Section, Det 1, 533 TRS, Falcon AFB, CO. He entered the Graduate Space Operations program at the Air Force Institute of Technology in May 1996. His next assignment is to Air Force Space Command Headquarters at Peterson AFB, CO.

Permanent Address: 1003 Havenwood Dr.
Libertyville, IL 60048

REPORT DOCUMENTATION PAGE

Form Approved
OMB No. 0704-0188

1. AGENCY USE ONLY *(Leave blank)*	2. REPORT DATE	3. REPORT TYPE AND DATES COVERED
	December 1997	Master's Thesis

4. TITLE AND SUBTITLE
Optimal Non-coplanar Launch
To Quick Rendezvous

5. FUNDING NUMBERS

6. AUTHOR(S)
Gregory B. Sears, Capt, USAF

7. PERFORMING ORGANIZATION NAME(S) AND ADDRESS(ES)
Air Force Institute of Technology, WPAFB OH 45433-6583

8. PERFORMING ORGANIZATION REPORT NUMBER
AFIT/GSO/ENY/97D-03

9. SPONSORING / MONITORING AGENCY NAME(S) AND ADDRESS(ES)
Lt Col Jess Sponable
Phillips Lab/VT-X
3515 Aberdeen Ave.
Kirtland AFB, NM 87117

10. SPONSORING / MONITORING AGENCY REPORT NUMBER

11. SUPPLEMENTARY NOTES

12a. DISTRIBUTION / AVAILABILITY STATEMENT
Approved for public release; distribution unlimited

12b. DISTRIBUTION CODE
A

13. ABSTRACT *(Maximum 200 words)*

The purpose of this study was to determine the feasibility of launching a Delta Clipper-like vehicle on an optimal, non-coplanar trajectory to rendezvous with an earth orbiting object in one orbit or less. The focus of the research was to determine what such a trajectory would look like, and to determine the cost, in payload mass, of flying such a trajectory. A model for the ascent trajectory was developed using the dynamics equations of motion, an atmosphere model, and an aerodynamic model for the DC-Y concept vehicle. A boundary value problem was posed and solved for a coplanar rendezvous. The non-coplanar solutions were obtained through extrapolation from the coplanar solution.

14. SUBJECT TERMS
Launch, Rendezvous, Non-coplanar, Trajectories, Delta Clipper, Optimization

15. NUMBER OF PAGES
77

16. PRICE CODE

17. SECURITY CLASSIFICATION OF REPORT	18. SECURITY CLASSIFICATION OF THIS PAGE	19. SECURITY CLASSIFICATION OF ABSTRACT	20. LIMITATION OF ABSTRACT
Unclassified	Unclassified	Unclassified	UL